

Incompressible Navier-Stokes Solver

Danial Rezaee¹

Project information:

Course:

*Computational Fluid
Dynamics*

Project No.:

No. 4

Professor:

*Dr. A. Nejat*¹

Student No.:

810600196

Created:

July 2022

Abstract

In this project we have solved the *Navier-Stokes* Equation for a cavity flow inside a box with a moving top and a flow inside a duct. Both cases have similar governing equations but different boundary conditions. Implicit Approximate Factorization method and Explicit RK-4 has been used to solve the equations from the discretized domain using Finite Volume Method. In the beginning the correctness of implicit discretization of the Navier-Stokes equation has been examined, then it has been checked whether the chosen time step and discretization method is stable, at the end the number of Iterations for convergence and accuracy of each method for both flows has been compared. A *python* program has been written to solve this problem.

1 Problem Description

1.1 Governing Equations

The system of equations to be solved is *Continuity* plus *x* and *y Momentum* equations in the non-dimensional form:

$$\text{Continuity : } \frac{\partial u}{\partial x} + \frac{\partial v}{\partial y} \quad (1)$$

$$x - \text{Momentum : } \frac{\partial u}{\partial t} + \frac{\partial u^2}{\partial x} + \frac{\partial uv}{\partial y} = -\frac{\partial p}{\partial x} + \frac{1}{Re} \left(\frac{\partial^2 u}{\partial x^2} + \frac{\partial^2 u}{\partial y^2} \right) \quad (2)$$

$$y - \text{Momentum : } \frac{\partial v}{\partial t} + \frac{\partial uv}{\partial x} + \frac{\partial v^2}{\partial y} = -\frac{\partial p}{\partial y} + \frac{1}{Re} \left(\frac{\partial^2 v}{\partial x^2} + \frac{\partial^2 v}{\partial y^2} \right) \quad (3)$$

1.2 Solution Domain

1.2.1 Cavity Flow

This case is a flow inside a box with a moving lid:

¹School of Mechanical Engineering, College of Engineering, University of Tehran, Tehran, Iran

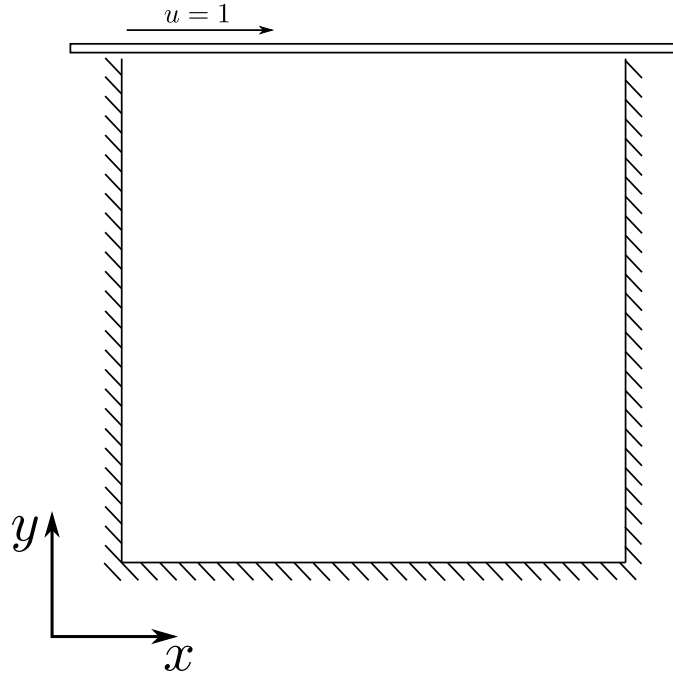


Figure 1: Cavity Flow sketch

For this geometry we will solve Eq.s(1,2,3) for the following boundary conditions and geometrical dimensions:

1.2.1.1 Nonmoving Lid Square Box As the title says in this case $U = 0$, and the width and height of the box are equal and equivalent to unity,

Boundary conditions:

$$\left\{ \begin{array}{ll} @ y = 0 & ; u = v = 0 \\ @ y = 1 & ; u = v = 0 \\ @ x = 0 & ; u = v = 0 \\ @ x = 1 & ; u = v = 0 \end{array} \right. \quad (4)$$

Geometrical dimensions:

$$w = h = 1 \quad (5)$$

where w is *width* and h is *height* of the box.

This case will be solved for validation and stability check.

1.2.1.2 Moving Lid Square Box In this case the lid is moving with velocity $U = 1$, and height of the box are equal and equivalent to unity,

$$\left\{ \begin{array}{ll} @ y = 0 & ; u = v = 0 \\ @ y = 1 & ; u = 1, v = 0 \\ @ x = 0 & ; u = v = 0 \\ @ x = 1 & ; u = v = 0 \end{array} \right. \quad (6)$$

Geometrical dimensions:

$$w = h = 1 \quad (7)$$

where w is *width* and h is *height* of the box.

1.2.1.3 Moving Lid in Opposite Direction Square Box In this case the lid is moving with velocity $U = -1$, and height of the box are equal and equivalent to unity,

$$\begin{cases} @ y = 0 & ; u = v = 0 \\ @ y = 1 & ; u = -1, v = 0 \\ @ x = 0 & ; u = v = 0 \\ @ x = 1 & ; u = v = 0 \end{cases} \quad (8)$$

Geometrical dimensions:

$$w = h = 1 \quad (9)$$

where w is *width* and h is *height* of the box.

This case is solved for checking if $u|_{U=1} + u|_{U=-1} \approx 0$, everywhere in the domain.

1.2.1.4 Moving Lid Rectangular Box In this case we have increased the height of the box to capture a second vortex in the flow, with the following boundary conditions and geometrical dimensions,

Boundary conditions:

$$\begin{cases} @ y = 0 & ; u = v = 0 \\ @ y = 3 & ; u = 1, v = 0 \\ @ x = 0 & ; u = v = 0 \\ @ x = 1 & ; u = v = 0 \end{cases} \quad (10)$$

Geometrical dimensions:

$$\begin{cases} w = 1 \\ h = 3 \end{cases} \quad (11)$$

1.2.2 Duct Flow

In this case we will solve a flow inside a duct. The inlet uniform velocity of $U = 1$ is set as the velocity inlet and the outlet pressure is $p = 0$ as the gauge atmospheric pressure. The length and height of the duct are set to be 8 and 1 (everything is non-dimensional). The fixed pressure and fully developed condition are set as the outlet boundary conditions,

Boundary conditions:

$$\begin{cases} @ x = 0 & ; u = U_{in} = 1, v = 0 \\ @ x = 8 & ; \frac{\partial u}{\partial x}|_{x=8} = 0 ; \frac{\partial v}{\partial x}|_{x=8} = 0 \\ @ y = 0 & ; u = v = 0 \\ @ y = 1 & ; u = v = 0 \\ @ x = 8 & ; p = 0 \end{cases} \quad (12)$$

Geometrical dimensions:

$$\begin{cases} L = 8 \\ h = 1 \end{cases} \quad (13)$$

2 Artificial Compressibility Method

As you see the continuity Eq.(1) has no linkage with momentum equations Eq.s (2, 3), in *Artificial Compressibility Methods*. a non-physical pressure time derivative called *Pseudo Compressibility*, is added to the continuity Eq.(1). That time derivative of pressure makes the necessary linkage between continuity and momentum Eq.s (2, 3):

$$\text{Continuity : } \beta \frac{\partial p}{\partial t} + \frac{\partial u}{\partial x} + \frac{\partial v}{\partial y} \quad (14)$$

$$x - \text{Momentum : } \frac{\partial u}{\partial t} + \frac{\partial u^2}{\partial x} + \frac{\partial uv}{\partial y} = -\frac{\partial p}{\partial x} + \frac{1}{Re} \left(\frac{\partial^2 u}{\partial x^2} + \frac{\partial^2 u}{\partial y^2} \right) \quad (15)$$

$$y - \text{Momentum : } \frac{\partial v}{\partial t} + \frac{\partial uv}{\partial x} + \frac{\partial v^2}{\partial y} = -\frac{\partial p}{\partial y} + \frac{1}{Re} \left(\frac{\partial^2 v}{\partial x^2} + \frac{\partial^2 v}{\partial y^2} \right) \quad (16)$$

The coefficient β is used to scale the effect of Pseudo Compressibility in modified set of Navier-Stokes Eq.s (14, 15, 16).

choosing small β s or $\beta \rightarrow 0$ looses the coupling of the continuity and momentum equations, and choice of large β increases the coupling between the equations. In fact β tunes the pressure wave propagation speed in the domain in solution process. In real case, and for incompressible Navier-Stokes, the speed of pressure wave propagation is very very large compared to velocity field and it is considered infinite. Therefore, the pressure time derivative in real Incompressible Navier-Stokes (INS) is negligible or zero.

3 Vector Form of Governing Equations

The INS set of Eq.s (14, 15, 16) can be recast in vector flux format:

$$\frac{\partial U}{\partial t} + \frac{\partial F}{\partial x} + \frac{\partial G}{\partial y} = 0 \quad (17)$$

Where:

$$U = \begin{pmatrix} p \\ u \\ v \end{pmatrix} \quad (18)$$

$$F = \begin{pmatrix} \frac{u}{\beta} \\ u^2 + p - \frac{1}{Re} \frac{\partial u}{\partial x} \\ uv - \frac{1}{Re} \frac{\partial v}{\partial x} \end{pmatrix} \quad (19)$$

$$G = \begin{pmatrix} \frac{v}{\beta} \\ uv - \frac{1}{Re} \frac{\partial u}{\partial y} \\ v^2 + p - \frac{1}{Re} \frac{\partial v}{\partial y} \end{pmatrix} \quad (20)$$

U is called *Solution Vector*, and F and G are *Flux Vectors* in x and y directions.

We can write Eq.(17) in the following form:

$$\frac{\partial U}{\partial t} + \nabla \mathbf{F} = 0 \quad (21)$$

Where \mathbf{F} is:

$$\mathbf{F} = F\hat{\mathbf{i}} + G\hat{\mathbf{j}} \quad (22)$$

4 Domain Discretization

Integrating Eq.(21) and using Gauss theorem we get:

$$\frac{dU_{i,j}}{dt} + \frac{F_{i+\frac{1}{2},j} - F_{i-\frac{1}{2},j}}{\Delta x} + \frac{G_{i,j+\frac{1}{2}} - G_{i,j-\frac{1}{2}}}{\Delta y} = 0 \quad (23)$$

Eq.(23) can be integrated in time explicitly using explicit time integration method such as *Explicit Euler*:

$$\frac{U_{i,j}^{m+1} - U_{i,j}^m}{\Delta t} = -\frac{F_{i+\frac{1}{2},j}^m - F_{i-\frac{1}{2},j}^m}{\Delta x} - \frac{G_{i,j+\frac{1}{2}}^m - G_{i,j-\frac{1}{2}}^m}{\Delta y} \quad (24)$$

Not surprisingly it is possible to solve INS explicitly, however the convergence time is the penalty to pay as the convergence becomes very slow.

The alternative is to use implicit time advance, using implicit time advance for integration of Eq.(23) in time, we have:

$$\frac{U_{i,j}^{m+1} - U_{i,j}^m}{\Delta t} = -\frac{F_{i+\frac{1}{2},j}^{m+1} - F_{i-\frac{1}{2},j}^{m+1}}{\Delta x} - \frac{G_{i,j+\frac{1}{2}}^{m+1} - G_{i,j-\frac{1}{2}}^{m+1}}{\Delta y} \quad (25)$$

Now, we have to find the fluxes $F_{i+\frac{1}{2},j}$, $F_{i-\frac{1}{2},j}$, $G_{i,j+\frac{1}{2}}$, and $G_{i,j-\frac{1}{2}}$ at time level $m+1$. To do so, we linearize the flux functions in time.

For instance, flux $F_{i+\frac{1}{2},j}$ can be expressed using the solution vectors Eq.(18) of $U_{i,j}$ and $U_{i+1,j}$:

$$F_{i+\frac{1}{2},j}^{m+1} = F_{i+\frac{1}{2},j}(U_{i,j}^{m+1}, U_{i+1,j}^{m+1}) = F_{i+\frac{1}{2},j}(U_{i,j}^m + \delta U_{i,j}^{m+1}, U_{i+1,j}^m + \delta U_{i+1,j}^{m+1}) \quad (26)$$

The flux function F , then is linearized as following:

$$F_{i+\frac{1}{2},j}^{m+1} = F_{i+\frac{1}{2},j}(U_{i,j}^m, U_{i+1,j}^m) + \left. \frac{\partial F_{i+\frac{1}{2},j}}{\partial U_{i,j}} \right|^m \delta U_{i,j}^{m+1} + \left. \frac{\partial F_{i+\frac{1}{2},j}}{\partial U_{i+1,j}} \right|^m \delta U_{i+1,j}^{m+1} + O(\delta U)^2 \quad (27)$$

Similarly $G_{i,j-\frac{1}{2}}^{m+1}$ can be expressed as following:

$$G_{i,j-\frac{1}{2}}^{m+1} = G_{i,j-\frac{1}{2},j}(U_{i,j-1}^m, U_{i,j}^m) + \left. \frac{\partial G_{i,j-\frac{1}{2}}}{\partial U_{i,j-1}} \right|^m \delta U_{i,j-1}^{m+1} + \left. \frac{\partial G_{i,j-\frac{1}{2}}}{\partial U_{i,j}} \right|^m \delta U_{i,j}^{m+1} + O(\delta U)^2 \quad (28)$$

We can find the proper expressions for $F_{i-\frac{1}{2},j}^{m+1}$ and $G_{i,j+\frac{1}{2}}^{m+1}$ in similar way, and Eq.(25) is expanded based on linearization of the fluxes in time:

$$\begin{aligned} \frac{U_{i,j}^{m+1} - U_{i,j}^m}{\Delta t} = & -\frac{1}{\Delta x} \left(F_{i+\frac{1}{2},j} + \left. \frac{\partial F_{i+\frac{1}{2},j}}{\partial U_{i,j}} \right|^m \delta U_{i,j}^{m+1} + \left. \frac{\partial F_{i+\frac{1}{2},j}}{\partial U_{i+1,j}} \right|^m \delta U_{i+1,j}^{m+1} \right) \\ & + \frac{1}{\Delta x} \left(F_{i-\frac{1}{2},j} + \left. \frac{\partial F_{i-\frac{1}{2},j}}{\partial U_{i-1,j}} \right|^m \delta U_{i-1,j}^{m+1} + \left. \frac{\partial F_{i-\frac{1}{2},j}}{\partial U_{i,j}} \right|^m \delta U_{i,j}^{m+1} \right) \\ & - \frac{1}{\Delta y} \left(G_{i,j+\frac{1}{2}} + \left. \frac{\partial G_{i,j+\frac{1}{2}}}{\partial U_{i,j}} \right|^m \delta U_{i,j}^{m+1} + \left. \frac{\partial G_{i,j+\frac{1}{2}}}{\partial U_{i,j+1}} \right|^m \delta U_{i,j+1}^{m+1} \right) \\ & + \frac{1}{\Delta y} \left(G_{i,j-\frac{1}{2}} + \left. \frac{\partial G_{i,j-\frac{1}{2}}}{\partial U_{i,j-1}} \right|^m \delta U_{i,j-1}^{m+1} + \left. \frac{\partial G_{i,j-\frac{1}{2}}}{\partial U_{i,j}} \right|^m \delta U_{i,j}^{m+1} \right) \end{aligned} \quad (29)$$

Arranging Eq.(29), bringing everything related to $m+1$ time step to the left and leaving all terms at time step m at the right hand side (RHS), we get:

$$\begin{aligned} & \left\{ \left(\frac{I}{\Delta t} + \frac{1}{\Delta x} \left. \frac{\partial F_{i+\frac{1}{2},j}}{\partial U_{i,j}} \right|^m - \frac{1}{\Delta x} \left. \frac{\partial F_{i-\frac{1}{2},j}}{\partial U_{i,j}} \right|^m + \frac{1}{\Delta y} \left. \frac{\partial G_{i,j+\frac{1}{2}}}{\partial U_{i,j}} \right|^m - \frac{1}{\Delta y} \left. \frac{\partial G_{i,j-\frac{1}{2}}}{\partial U_{i,j}} \right|^m \right) \delta U_{i,j}^{m+1} \right. \\ & + \left. \frac{1}{\Delta x} \left. \frac{\partial F_{i+\frac{1}{2},j}}{\partial U_{i+1,j}} \right|^m \delta U_{i+1,j}^{m+1} - \frac{1}{\Delta x} \left. \frac{\partial F_{i-\frac{1}{2},j}}{\partial U_{i-1,j}} \right|^m \delta U_{i-1,j}^{m+1} + \frac{1}{\Delta y} \left. \frac{\partial G_{i,j+\frac{1}{2}}}{\partial U_{i,j+1}} \right|^m \delta U_{i,j+1}^{m+1} - \frac{1}{\Delta y} \left. \frac{\partial G_{i,j-\frac{1}{2}}}{\partial U_{i,j-1}} \right|^m \delta U_{i,j-1}^{m+1} \right\} \\ & = -\frac{F_{i+\frac{1}{2},j}^m - F_{i-\frac{1}{2},j}^m}{\Delta x} - \frac{G_{i,j+\frac{1}{2}}^m - G_{i,j-\frac{1}{2}}^m}{\Delta y} \equiv RHS_{i,j} \end{aligned} \quad (30)$$

So far we have described everything except the evaluation of fluxes at the faces of control volume (i, j) such as $F_{i+\frac{1}{2},j}$, $G_{i,j-\frac{1}{2}}$, ..., and the computation of derivatives of such fluxes respect to solution variables, i.e., $\frac{\partial F_{i+\frac{1}{2},j}}{\partial U_{i,j}}$, $\frac{\partial G_{i,j-\frac{1}{2}}}{\partial U_{i,j-1}}$,

For computing the fluxes, we use either central averaging or central differencing, For example for $F_{i+\frac{1}{2},j}$, we can write:

$$U_{i,j} = \begin{pmatrix} p_{i,j} \\ u_{i,j} \\ v_{i,j} \end{pmatrix} \quad (31)$$

$$U_{i+1,j} = \begin{pmatrix} p_{i+1,j} \\ u_{i+1,j} \\ v_{i+1,j} \end{pmatrix} \quad (32)$$

$$F_{i+\frac{1}{2},j} = \begin{pmatrix} \frac{u_{i+\frac{1}{2},j}}{\beta} \\ u_{i+\frac{1}{2},j}^2 + p_{i+\frac{1}{2},j} - \frac{1}{Re} \frac{\partial u}{\partial x} \Big|_{i+\frac{1}{2},j} \\ u_{i+\frac{1}{2},j} v_{i+\frac{1}{2},j} - \frac{1}{Re} \frac{\partial v}{\partial x} \Big|_{i+\frac{1}{2},j} \end{pmatrix} \quad (33)$$

Using central averaging and differencing we get:

$$\begin{cases} p_{i+\frac{1}{2},j} = \frac{p_{i,j} + p_{i+1,j}}{2} ; & \frac{\partial u}{\partial x} \Big|_{i+\frac{1}{2},j} = \frac{u_{i+1,j} - u_{i,j}}{\Delta x} \\ u_{i+\frac{1}{2},j} = \frac{u_{i,j} + u_{i+1,j}}{2} \\ v_{i+\frac{1}{2},j} = \frac{v_{i,j} + v_{i+1,j}}{2} ; & \frac{\partial v}{\partial x} \Big|_{i+\frac{1}{2},j} = \frac{v_{i+1,j} - v_{i,j}}{\Delta x} \end{cases} \quad (34)$$

Finally we have:

$$F_{i+\frac{1}{2},j} = \begin{pmatrix} \frac{u_{i+1,j} + u_{i,j}}{2\beta} \\ \left(\frac{u_{i+1,j} + u_{i,j}}{2} \right)^2 + \frac{p_{i+1,j} + p_{i,j}}{2} - \frac{1}{Re} \frac{u_{i+1,j} - u_{i,j}}{\Delta x} \\ \left(\frac{u_{i+1,j} + u_{i,j}}{2} \right) \left(\frac{v_{i+1,j} + v_{i,j}}{2} \right) - \frac{1}{Re} \frac{v_{i+1,j} - v_{i,j}}{\Delta x} \end{pmatrix} \quad (35)$$

Similarly, we can evaluate $G_{i,j-\frac{1}{2}}$:

$$G_{i,j-\frac{1}{2}} = \begin{pmatrix} \frac{v_{i,j-1} + v_{i,j}}{2\beta} \\ \left(\frac{u_{i,j-1} + u_{i,j}}{2} \right) \left(\frac{v_{i,j} + v_{i,j-1}}{2} \right) - \frac{1}{Re} \frac{u_{i,j} - u_{i,j-1}}{\Delta y} \\ \left(\frac{v_{i,j-1} + v_{i,j}}{2} \right)^2 + \frac{p_{i,j-1} + p_{i,j}}{2} - \frac{1}{Re} \frac{v_{i,j} - v_{i,j-1}}{\Delta y} \end{pmatrix} \quad (36)$$

The derivative of flux vector respect to solution variables are called *Jacobian Matrices*. To compute the Jacobian Matrix the derivative of each row of the flux vector is taken respect to all rows of the solution vector, and the derivatives are put in a matrix with the same row arrangement of the flux velocity and the column index of the solution variable, i.e.:

$$F = \begin{pmatrix} F_1 \\ F_2 \\ F_3 \end{pmatrix} ; G = \begin{pmatrix} G_1 \\ G_2 \\ G_3 \end{pmatrix} ; \frac{\partial F}{\partial U} = \begin{pmatrix} \frac{\partial F_1}{\partial U_1} & \frac{\partial F_1}{\partial U_2} & \frac{\partial F_1}{\partial U_3} \\ \frac{\partial F_2}{\partial U_1} & \frac{\partial F_2}{\partial U_2} & \frac{\partial F_2}{\partial U_3} \\ \frac{\partial F_3}{\partial U_1} & \frac{\partial F_3}{\partial U_2} & \frac{\partial F_3}{\partial U_3} \end{pmatrix} \quad (37)$$

Here we have presented $\frac{\partial F_{i+\frac{1}{2},j}}{\partial U_{i,j}}$ and $\frac{\partial G_{i,j-\frac{1}{2}}}{\partial U_{i,j-1}}$ as the examples of the Jacobian terms of Eq.(30) which construct the *RHS* of the linear system to be solved to set the update values of $\delta U_{i,j}$ for the solution domain:

$$\frac{\partial F_{i+\frac{1}{2},j}}{\partial U_{i,j}} = \begin{pmatrix} 0 & \frac{1}{2\beta} & 0 \\ \frac{1}{2} \frac{u_{i,j} + u_{i+1,j}}{2} + \frac{1}{Re} \frac{1}{\Delta x} & & 0 \\ 0 & \frac{1}{2} \left(\frac{v_{i,j} + v_{i+1,j}}{2} \right) & \frac{1}{2} \left(\frac{u_{i,j} + u_{i+1,j}}{2} \right) + \frac{1}{Re} \frac{1}{\Delta x} \end{pmatrix} \quad (38)$$

and,

$$\frac{\partial G_{i,j-\frac{1}{2}}}{\partial U_{i,j-1}} = \begin{pmatrix} 0 & 0 & \frac{1}{2\beta} \\ 0 & \frac{1}{2} \left(\frac{v_{i,j} + v_{i,j-1}}{2} \right) + \frac{1}{Re} \frac{1}{\Delta y} & \frac{1}{2} \left(\frac{u_{i,j} + u_{i,j-1}}{2} \right) \\ \frac{1}{2} & 0 & \frac{v_{i,j} + v_{i,j-1}}{2} + \frac{1}{Re} \frac{1}{\Delta y} \end{pmatrix} \quad (39)$$

We can rewrite Eq.(30) as the following:

$$(I + \Delta t A_x E_{-1,0} + \Delta t B_x + \Delta t C_x E_{1,0} + \Delta t A_y E_{0,-1} + \Delta t B_y + \Delta t C_y E_{0,1}) \delta U_{i,j}^{m+1} = \Delta t R H S_{i,j} \quad (40)$$

Where, $E_{k,l} \delta U_{i,j} \equiv \delta U_{i+k,j+l}$ is called *Shift Operator*, and:

$$\begin{cases} A_x = -\frac{1}{\Delta x} \frac{\partial F_{i-\frac{1}{2},j}}{\partial U_{i,j}} \Big|_m, & B_x = \frac{1}{\Delta x} \frac{\partial F_{i+\frac{1}{2},j}}{\partial U_{i,j}} \Big|_m - \frac{1}{\Delta x} \frac{\partial F_{i-\frac{1}{2},j}}{\partial U_{i,j}} \Big|_m, & C_x = \frac{1}{\Delta x} \frac{\partial F_{i+\frac{1}{2},j}}{\partial U_{i+1,j}} \Big|_m \\ A_y = -\frac{1}{\Delta y} \frac{\partial G_{i,j-\frac{1}{2}}}{\partial U_{i,j-1}} \Big|^{m+1}, & B_y = \frac{1}{\Delta y} \frac{\partial G_{i,j+\frac{1}{2}}}{\partial U_{i,j}} \Big|^{m+1} - \frac{1}{\Delta y} \frac{\partial G_{i,j-\frac{1}{2}}}{\partial U_{i,j}} \Big|^{m+1}, & C_y = \frac{1}{\Delta y} \frac{\partial G_{i,j+\frac{1}{2}}}{\partial U_{i,j+1}} \Big|^{m+1} \end{cases} \quad (41)$$

Eq.(40) is a *Five Block Diagonal* linear system that needs to be solved at each time level to get an update for $\delta U_{i,j}^{m+1}$, for the solution domain. Since the Navier-Stokes equation is non-linear we may need many iterations before reaching the steady-state solution, where $\delta U_{i,j}^{m+1} = 0$ or $R H S_{i,j} = 0$, therefore we factor Eq.(40) into two *Three-Block Diagonal* linear systems.

5 Approximate Factorization

Eq.(40) is approximately factored to Eq.(42), using ADI technique:

$$(I + \Delta t A_x E_{-1,0} + \Delta t B_x + \Delta t C_x E_{1,0}) (I + \Delta t A_y E_{0,-1} + \Delta t B_y + \Delta t C_y E_{0,1}) \delta U_{i,j}^{m+1} = \Delta t R H S_{i,j} \quad (42)$$

And Eq.(42) is solved using ADI technique over solution domain. Solving Eq.(42), involves solving two systems of three-block diagonal matrices, which is way more easier than solving the Eq.(40) itself.

$$(I + \Delta t A_x E_{-1,0} + \Delta t B_x + \Delta t C_x E_{1,0}) \delta \tilde{U}_{i,j} = \Delta t R H S_{i,j} \quad (43)$$

$$(I + \Delta t A_y E_{0,-1} + \Delta t B_y + \Delta t C_y E_{0,1}) \delta U_{i,j}^{m+1} = \delta \tilde{U}_{i,j} \quad (44)$$

Solve Eq.(43) to get $\delta \tilde{U}_{i,j}$ and then solve Eq.(44) to find $\delta U_{i,j}^{m+1}$. Update the solution to find $U_{i,j}^{m+1}$, repeat the process till $R H S_{i,j}$ becomes zero, which means the flux integral of the cell (i, j) is fully satisfied and the solution variables are converged to the steady-state solution.

6 Boundary Conditions for Navier-Stokes Equations

6.1 Wall Boundary Conditions

There is no difference between the velocity of the fluid and the wall adjacent to each other:

$$\begin{cases} u_{fluid} = u_{wall} \\ v_{fluid} = v_{wall} \end{cases} \quad (45)$$

However for the pressure, we need to do some calculation and approximation. We write the momentum equation normal to the wall (e.g., Eq.(3)):

$$\frac{\partial \mathcal{X}}{\partial t} + \frac{\partial \mathcal{U}\mathcal{X}}{\partial x} + \frac{\partial v^2}{\partial y} = -\frac{\partial p}{\partial y} + \frac{1}{Re} \left(\frac{\partial^2 \mathcal{X}}{\partial x^2} + \frac{\partial^2 v}{\partial y^2} \right) \quad (46)$$

u and v are zeros at the wall at all xs and ts , therefore the momentum Eq.(46) is simplified to:

$$\frac{\partial v^2}{\partial y} = -\frac{\partial p}{\partial y} + \frac{1}{Re} \frac{\partial^2 v}{\partial y^2} \quad (47)$$

Using continuity Eq.(1) on the wall and knowing that u is zero at all xs , we can show $\frac{\partial v^2}{\partial y} = 0$, so:

$$\frac{\partial p}{\partial y} = \frac{1}{Re} \frac{\partial^2 v}{\partial y^2} \quad (48)$$

Although $\frac{\partial^2 v}{\partial y^2}$ is not essentially zero, however, generally it is very small, particularly for straight walls. Therefore, we may use $\frac{\partial p}{\partial y} = 0$.

Therefore, we can summarize the wall boundary conditions for INS as the following using ghost cells.

6.1.1 Stationary Wall

$$\begin{cases} u_w = \frac{u_{i,0} + u_{i,1}}{2} = 0 \\ v_w = \frac{v_{i,0} + v_{i,1}}{2} = 0 \\ \left. \frac{\partial p}{\partial y} \right|_w = \frac{p_{i,1} - p_{i,0}}{\Delta y} = 0 \end{cases} \quad (49)$$

or,

$$\begin{cases} u_{i,0} = -u_{i,1} \\ v_{i,0} = -v_{i,1} \\ p_{i,0} = p_{i,1} \end{cases} \quad (50)$$

These conditions are valid for all time levels, so, we can write the implicit form for the stationary wall boundary conditions (BC):

$$\begin{cases} \delta u_{i,0}^{m+1} + \delta u_{i,1}^{m+1} = 0 \\ \delta v_{i,0}^{m+1} + \delta v_{i,1}^{m+1} = 0 \\ \delta p_{i,0}^{m+1} - \delta p_{i,1}^{m+1} = 0 \end{cases} \quad (51)$$

6.1.2 Moving Wall

For moving Walls, the normal velocity is still zero, however, the tangential velocity is equal to the wall velocity. The pressure condition does not change:

$$\begin{cases} \frac{u_{i,0} + u_{i,1}}{2} = u_w \\ \frac{v_{i,0} + v_{i,1}}{2} = 0 \\ \left. \frac{\partial p}{\partial y} \right|_w = \frac{p_{i,1} - p_{i,0}}{\Delta y} = 0 \end{cases} \quad (52)$$

or,

$$\begin{cases} u_{i,0} = 2u_w - u_{i,1} \\ v_{i,0} = -v_{i,1} \\ p_{i,0} = p_{i,1} \end{cases} \quad (53)$$

Also we can derive the implicit formulation for moving walls, the normal velocity component and the pressure boundaries are similar to those of stationary wall:

$$\begin{cases} \delta u_{i,0}^{m+1} + \delta u_{i,1}^{m+1} = 0 \\ \delta v_{i,0}^{m+1} + \delta v_{i,1}^{m+1} = 0 \\ \delta p_{i,0}^{m+1} - \delta p_{i,1}^{m+1} = 0 \end{cases} \quad (54)$$

6.2 Inflow Boundary Conditions

For incompressible Navier-Stokes, we need to set the mass flux at the inlet. This is done by setting u , v or \vec{V} at the inlet. The pressure itself can not be set at the inflow, but assuming fully developed entrance, we can find an expression for pressure-gradient at the entrance using x -momentum Eq.(2). Since the flow is fully-developed (internal flow), v must be zero and u is not changing with x at the entrance. We accept the fact, that flow may not be quite developed at the entrance, however, we can neglect that effect on the pressure gradient.

$$\left. \frac{\partial p}{\partial x} \right|_{in} = \frac{1}{Re} \frac{\partial^2 u}{\partial y^2} \quad (55)$$

The right hand side of the simplified x -momentum Eq.(55) can be computed either using entrance boundary profile or even the first interior cell (i.e., $i = 1$).

$$\begin{cases} u_{in} = \frac{u_{0,j} + u_{1,j}}{2} \\ v_{0,j} = -v_{1,j} \\ \frac{p_{1,j} - p_{0,j}}{\Delta x} = \left. \frac{\partial p}{\partial x} \right|_{in} \end{cases} \quad (56)$$

or,

$$\begin{cases} u_{0,j} = 2u_{in} - u_{1,j} \\ v_{0,j} = -v_{1,j} \\ p_{0,j} = p_{1,j} - \Delta x \left. \frac{\partial p}{\partial x} \right|_{in} \end{cases} \quad (57)$$

The implicit boundary conditions for inflow can be formulated as:

$$\begin{cases} \delta u_{0,j}^{m+1} + \delta u_{1,j}^{m+1} = 0 \\ \delta v_{0,j}^{m+1} + \delta v_{1,j}^{m+1} = 0 \\ \delta p_{0,j}^{m+1} - \delta p_{1,j}^{m+1} = 0 \end{cases} \quad (58)$$

6.3 Outflow Boundary Conditions

For INS, the outlet pressure must be fixed and generally is set to p_∞ . The reasonable condition for velocity is the fully developed flow with no stream wise velocity gradient:

$$\begin{cases} u_{imax+1,j} = u_{imax,j} \\ v_{imax+1,j} = v_{imax,j} \\ p_{imax+1,j} = 2p_\infty - p_{imax,j} \end{cases} \quad (59)$$

The implicit boundary condition for outflow can be formulated as:

$$\begin{cases} \delta u_{imax+1,j}^{m+1} - \delta u_{imax,j}^{m+1} = 0 \\ \delta v_{imax+1,j}^{m+1} - \delta v_{imax,j}^{m+1} = 0 \\ \delta p_{imax+1,j}^{m+1} + \delta p_{imax,j}^{m+1} = 0 \end{cases} \quad (60)$$

If the length of the flow domain is not enough for fully developing flow, enforcing zero gradient on velocity at the outlet may not physically be correct but it is needed to compute the flow field numerically, since we need to limit effect of the outlet boundary on the interior domain, letting the flow to exit the domain smoothly.

7 General Validation

7.1 Correctness of Residual

Consider a square geometry on $[0, 1] \times [0, 1]$ with no-slip boundary conditions and the following distribution of velocity and pressure:

$$\begin{pmatrix} p \\ u \\ v \end{pmatrix} = \begin{pmatrix} p_0 \cos(\pi x) \cos(\pi y) \\ u_0 \sin(\pi x) \sin(2\pi y) \\ v_0 \sin(2\pi x) \sin(\pi y) \end{pmatrix} \quad (61)$$

Note that this data satisfies the boundary conditions. The exact flux integral divided by the cell size is given by:

$$-\frac{\partial F}{\partial x} - \frac{\partial G}{\partial y} = \begin{pmatrix} -\frac{\pi}{\beta} (u_0 C_x S_{2y} + v_0 S_{2x} C_y) \\ p_0 \pi S_x C_y - u_0^2 \pi S_{2x} S_{2y}^2 - u_0 v_0 \pi S_x S_{2x} (C_y S_{2y} + 2C_{2y} S_y) - u_0 \frac{5\pi^2 S_x S_{2y}}{Re} \\ p_0 \pi C_x S_y - v_0^2 \pi S_{2x} S_{2y}^2 - u_0 v_0 \pi S_y S_{2y} (C_x S_{2x} + 2C_{2x} S_x) - v_0 \frac{5\pi^2 S_{2x} S_y}{Re} \end{pmatrix} \quad (62)$$

Where:

$$\begin{cases} C_x = \cos(\pi x) \\ S_x = \sin(\pi x) \\ C_y = \cos(\pi y) \\ S_y = \sin(\pi y) \\ C_{2x} = \cos(2\pi x) \\ S_{2x} = \sin(2\pi x) \\ C_{2y} = \cos(2\pi y) \\ S_{2y} = \sin(2\pi y) \end{cases} \quad (63)$$

We now compute the flux integral analytically Eq.(62) and numerically using right-hand side of Eq.(30) on a 20×20 and a 40×40 mesh, setting u_0 , v_0 , and p_0 to 1, $\beta = 1$, $Re = 10$, $Re = 10^5$, $Re = 10^{-5}$ for the final calculation. For each case we compute L_2 norm of error and check if it is second-order accurate. In the Table.1 you can see the norm of errors of the flux integral:

Mesh size	Reynolds	B	L_{2p}	L_{2u}	L_{2v}
20×20	10.0	1	0.011983387844094969	0.05002585519060251	0.05002585519060243
40×40	10.0	1	0.002995697655986389	0.012585866027593814	0.012585866027593833
20×20	1e-05	1	0.011983387844094969	17195.370390730666	17195.37039073067
40×40	1e-05	1	0.002995697655986389	4308.991423456004	4308.991423456006
20×20	100000.0	1	0.011983387844094969	0.048946971937080565	0.0489469719370805
40×40	100000.0	1	0.002995697655986389	0.012314797845527244	0.012314797845527232

Table 1: L_2 norm of the error in the flux integral

Now, we have to calculate the ratio of norm of errors for checking if it is second-order accurate:

Reynolds	$\frac{L_{2p} _{20 \times 20}}{L_{2p} _{40 \times 40}}$	$\frac{L_{2u} _{20 \times 20}}{L_{2u} _{40 \times 40}}$	$\frac{L_{2v} _{20 \times 20}}{L_{2v} _{40 \times 40}}$
10.0	4.000199359287216	3.974764635260187	3.974764635260175
1e-05	4.000199359287216	3.9905789315633426	3.9905789315633418
100000.0	4.000199359287216	3.974646807122229	3.9746468071222276

Table 2: Ratio of L_2 norms

As you see in Table.2 the ratio of L_2 norms is approximately 4, so, our flux integral is second-order accurate.

7.2 Correctness of Implicit Discretization Flux Jacobian Check

In this section we must show the correctness of the left-hand side (LHS) of Eq.(40), recall that the LHS arise from approximation that:

$$\left(\frac{F_{i+\frac{1}{2},j} - F_{i-\frac{1}{2},j}}{\Delta x} + \frac{G_{i,j+\frac{1}{2}} - G_{i,j-\frac{1}{2}}}{\Delta y} \right)^{m+1} - \left(\frac{F_{i+\frac{1}{2},j} - F_{i-\frac{1}{2},j}}{\Delta x} + \frac{G_{i,j+\frac{1}{2}} - G_{i,j-\frac{1}{2}}}{\Delta y} \right)^m \approx (I + \Delta t A_x E_{-1,0} + \Delta t B_x + \Delta t C_x E_{1,0} + \Delta t A_y E_{0,-1} + \Delta t B_y + \Delta t C_y E_{0,1}) \frac{\delta U_{i,j}}{\Delta t} \quad (64)$$

Suppose that for cell $(i, j) = (10, 10)$, we set:

$$\delta U_{i,j} = \begin{cases} 10^{-6} \begin{pmatrix} 1 \\ 1 \\ 1 \end{pmatrix} & ; \ i = j = 10 \\ 0 & ; \ otherwise \end{cases} \quad (65)$$

For a 20×20 mesh. Then, with $U_{i,j}^{m+1} = U_{i,j}^m + \delta U_{i,j}$, we can calculate all terms in the expansion. The error should be 10^{-10} or smaller:

Table 3: Pressure error for cell (10, 10) and $Re = 10$

Table 4: x -velocity component error for cell $(10, 10)$ and $Re = 10$

Table 4: x -velocity component error for cell $(10, 10)$ and $Re = 10$

0.0	0.0	0.0	0.0	0.0	0.0	0.0	0.0	0.0	0.0	0.0	0.0	0.0	0.0	0.0	0.0	0.0	0.0	0.0	0.0	0.0	0.0
0.0	0.0	0.0	0.0	0.0	0.0	0.0	0.0	0.0	0.0	0.0	0.0	0.0	0.0	0.0	0.0	0.0	0.0	0.0	0.0	0.0	0.0
0.0	0.0	0.0	0.0	0.0	0.0	0.0	0.0	0.0	0.0	0.0	0.0	0.0	0.0	0.0	0.0	0.0	0.0	0.0	0.0	0.0	0.0
0.0	0.0	0.0	0.0	0.0	0.0	0.0	0.0	0.0	0.0	0.0	0.0	0.0	0.0	0.0	0.0	0.0	0.0	0.0	0.0	0.0	0.0
0.0	0.0	0.0	0.0	0.0	0.0	0.0	0.0	0.0	0.0	0.0	0.0	0.0	0.0	0.0	0.0	0.0	0.0	0.0	0.0	0.0	0.0
0.0	0.0	0.0	0.0	0.0	0.0	0.0	0.0	0.0	0.0	0.0	0.0	0.0	0.0	0.0	0.0	0.0	0.0	0.0	0.0	0.0	0.0
0.0	0.0	0.0	0.0	0.0	0.0	0.0	0.0	0.0	0.0	0.0	0.0	0.0	0.0	0.0	0.0	0.0	0.0	0.0	0.0	0.0	0.0
0.0	0.0	0.0	0.0	0.0	0.0	0.0	0.0	0.0	0.0	0.0	0.0	0.0	0.0	0.0	0.0	0.0	0.0	0.0	0.0	0.0	0.0
0.0	0.0	0.0	0.0	0.0	0.0	0.0	0.0	0.0	0.0	0.0	0.0	0.0	0.0	0.0	0.0	0.0	0.0	0.0	0.0	0.0	0.0
0.0	0.0	0.0	0.0	0.0	0.0	0.0	0.0	0.0	0.0	0.0	0.0	0.0	0.0	0.0	0.0	0.0	0.0	0.0	0.0	0.0	0.0
0.0	0.0	0.0	0.0	0.0	0.0	0.0	0.0	0.0	0.0	0.0	0.0	0.0	0.0	0.0	0.0	0.0	0.0	0.0	0.0	0.0	0.0
0.0	0.0	0.0	0.0	0.0	0.0	0.0	0.0	0.0	0.0	0.0	4.99874675072981e-12	0.0	0.0	0.0	0.0	0.0	0.0	0.0	0.0	0.0	0.0
0.0	0.0	0.0	0.0	0.0	0.0	0.0	0.0	0.0	0.0	4.999944753472825e-12	2.064239621249464e-15	5.000202353132744e-12	0.0	0.0	0.0	0.0	0.0	0.0	0.0	0.0	0.0
0.0	0.0	0.0	0.0	0.0	0.0	0.0	0.0	0.0	0.0	0.0	4.999866582496189e-12	0.0	0.0	0.0	0.0	0.0	0.0	0.0	0.0	0.0	0.0
0.0	0.0	0.0	0.0	0.0	0.0	0.0	0.0	0.0	0.0	0.0	0.0	0.0	0.0	0.0	0.0	0.0	0.0	0.0	0.0	0.0	0.0
0.0	0.0	0.0	0.0	0.0	0.0	0.0	0.0	0.0	0.0	0.0	0.0	0.0	0.0	0.0	0.0	0.0	0.0	0.0	0.0	0.0	0.0
0.0	0.0	0.0	0.0	0.0	0.0	0.0	0.0	0.0	0.0	0.0	0.0	0.0	0.0	0.0	0.0	0.0	0.0	0.0	0.0	0.0	0.0
0.0	0.0	0.0	0.0	0.0	0.0	0.0	0.0	0.0	0.0	0.0	0.0	0.0	0.0	0.0	0.0	0.0	0.0	0.0	0.0	0.0	0.0
0.0	0.0	0.0	0.0	0.0	0.0	0.0	0.0	0.0	0.0	0.0	0.0	0.0	0.0	0.0	0.0	0.0	0.0	0.0	0.0	0.0	0.0
0.0	0.0	0.0	0.0	0.0	0.0	0.0	0.0	0.0	0.0	0.0	0.0	0.0	0.0	0.0	0.0	0.0	0.0	0.0	0.0	0.0	0.0
0.0	0.0	0.0	0.0	0.0	0.0	0.0	0.0	0.0	0.0	0.0	0.0	0.0	0.0	0.0	0.0	0.0	0.0	0.0	0.0	0.0	0.0
0.0	0.0	0.0	0.0	0.0	0.0	0.0	0.0	0.0	0.0	0.0	0.0	0.0	0.0	0.0	0.0	0.0	0.0	0.0	0.0	0.0	0.0
0.0	0.0	0.0	0.0	0.0	0.0	0.0	0.0	0.0	0.0	0.0	0.0	0.0	0.0	0.0	0.0	0.0	0.0	0.0	0.0	0.0	0.0
0.0	0.0	0.0	0.0	0.0	0.0	0.0	0.0	0.0	0.0	0.0	0.0	0.0	0.0	0.0	0.0	0.0	0.0	0.0	0.0	0.0	0.0
0.0	0.0	0.0	0.0	0.0	0.0	0.0	0.0	0.0	0.0	0.0	0.0	0.0	0.0	0.0	0.0	0.0	0.0	0.0	0.0	0.0	0.0
0.0	0.0	0.0	0.0	0.0	0.0	0.0	0.0	0.0	0.0	0.0	0.0	0.0	0.0	0.0	0.0	0.0	0.0	0.0	0.0	0.0	0.0
0.0	0.0	0.0	0.0	0.0	0.0	0.0	0.0	0.0	0.0	0.0	0.0	0.0	0.0	0.0	0.0	0.0	0.0	0.0	0.0	0.0	0.0

Table 5: y -velocity component error for cell $(10, 10)$ and $Re = 10$

As you see in Tables.(3, 4, 5), all errors are smaller than 10^{-5} .

8 Flow in a Box with a Moving Top

In this section we solve the Cavity Flow as it was described in Sec.1.2.1.

8.1 Validation Case: Stability

In this section we solve the Cavity Flow for a non-moving top as it was described in Sec.1.2.1.1, the calculations are done on a 20×20 mesh with $\Delta t = 0.05$ and $\beta = 1$.

We expect the velocity and pressure to be zero everywhere.

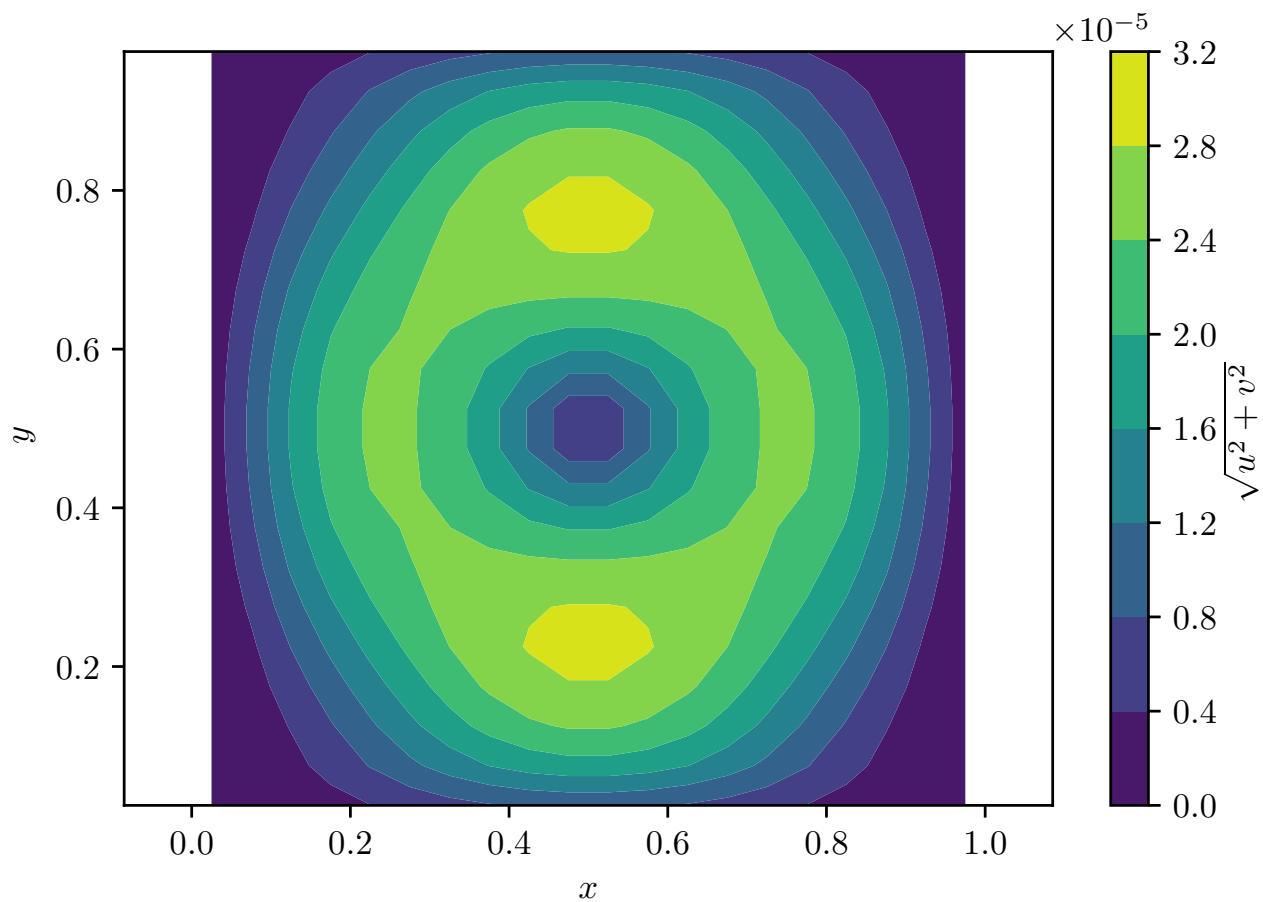


Figure 2: Absolute Velocity for $U = 0$, $\Delta t = 0.05$, and 20×20 mesh

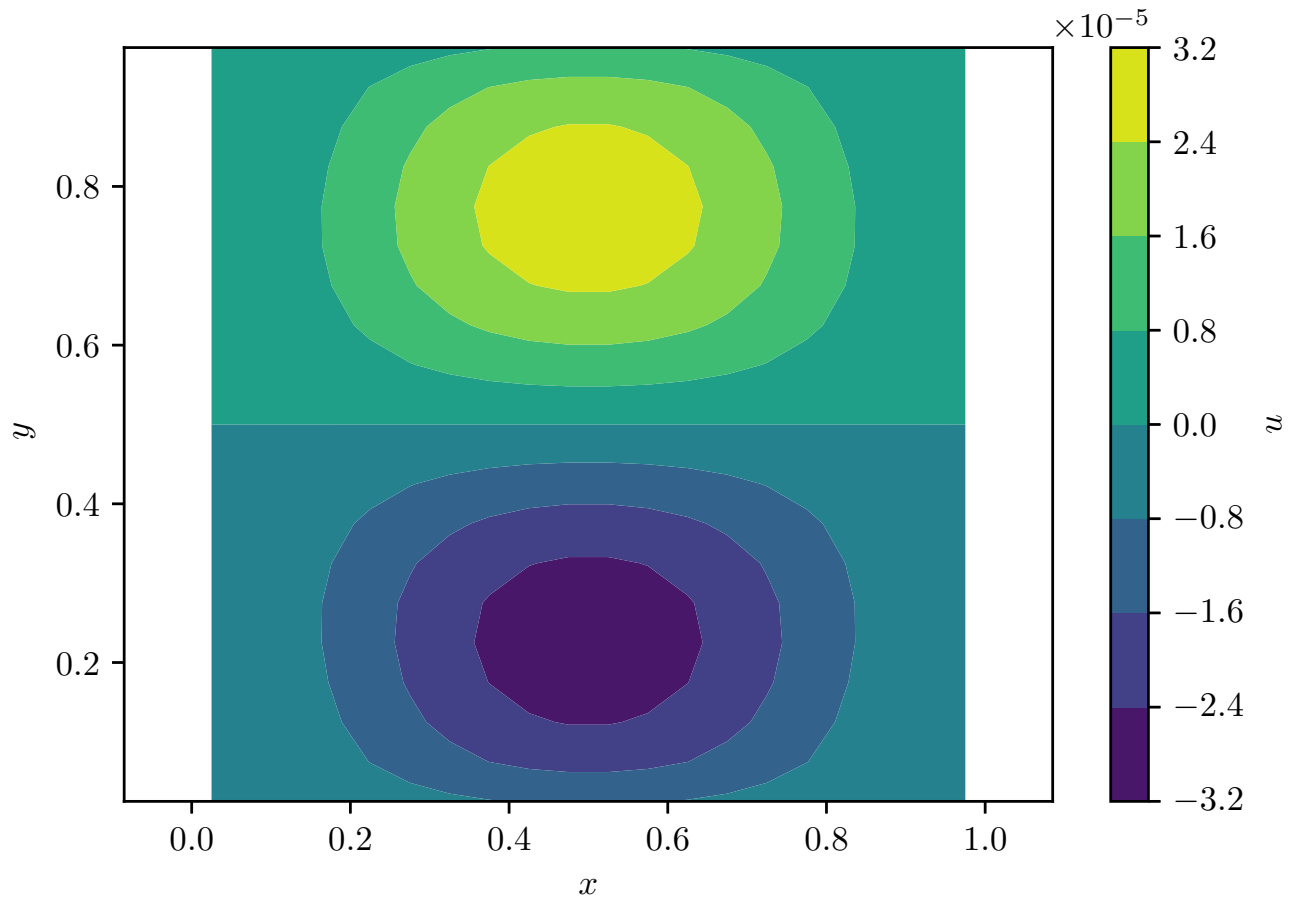


Figure 3: x -Velocity for $U = 0$, $\Delta t = 0.05$, and 20×20 mesh

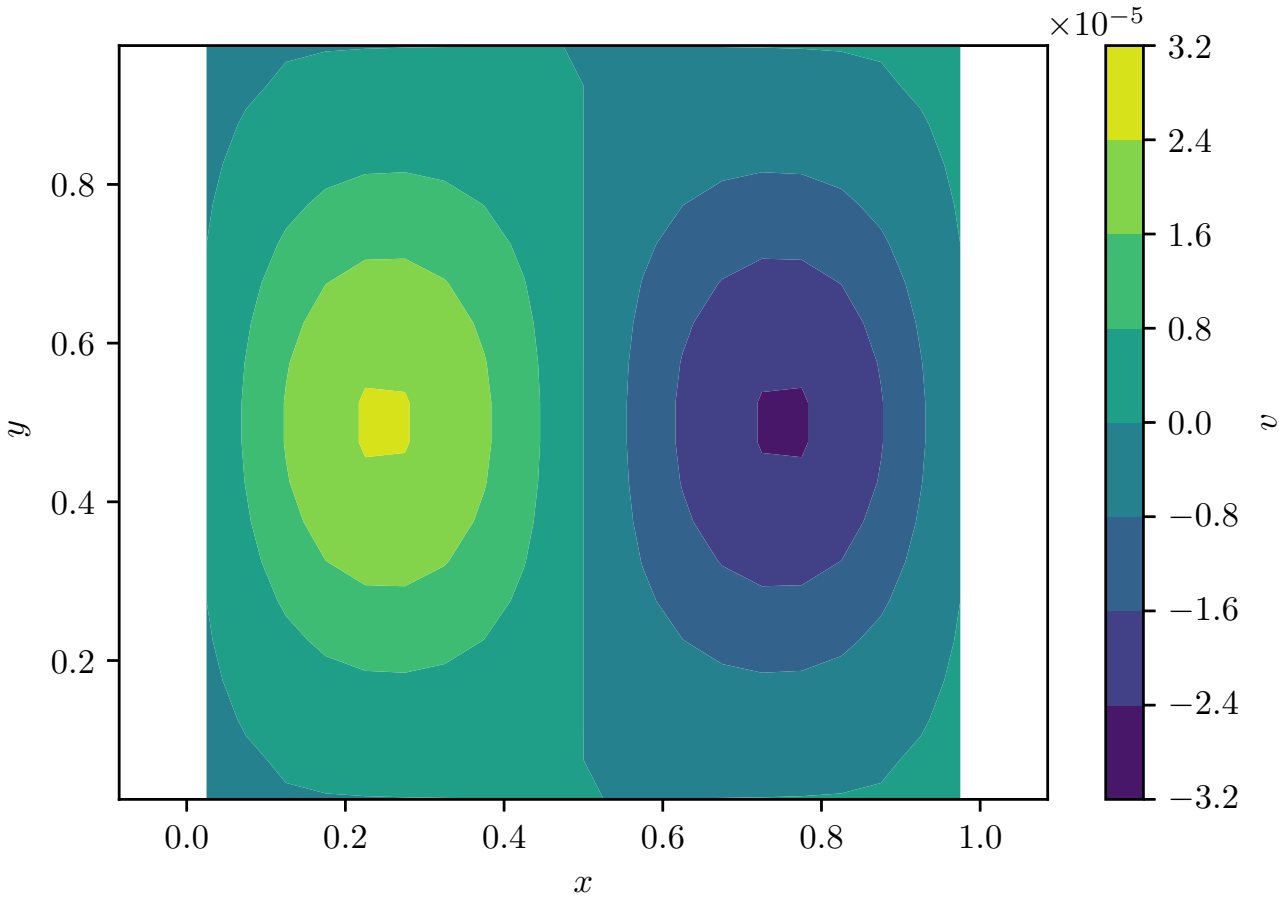


Figure 4: y -Velocity for $U = 0$, $\Delta t = 0.05$, and 20×20 mesh

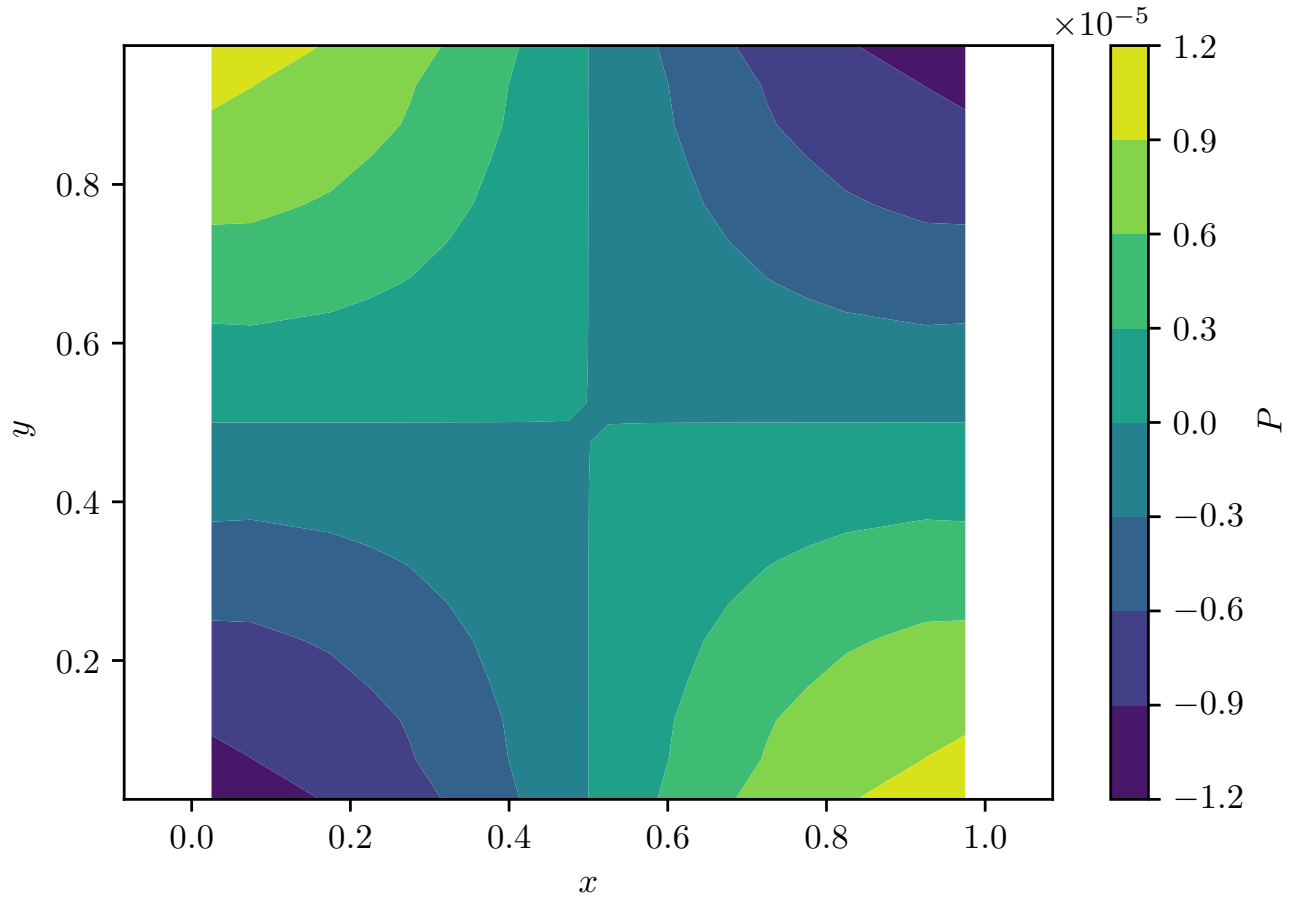


Figure 5: Pressure for $U = 0$, $\Delta t = 0.05$, and 20×20 mesh

As we expected and see in Figs 2, 3, 4, 5 the velocity and pressure are approximately zero (order 10^{-5}) everywhere in the solution domain.

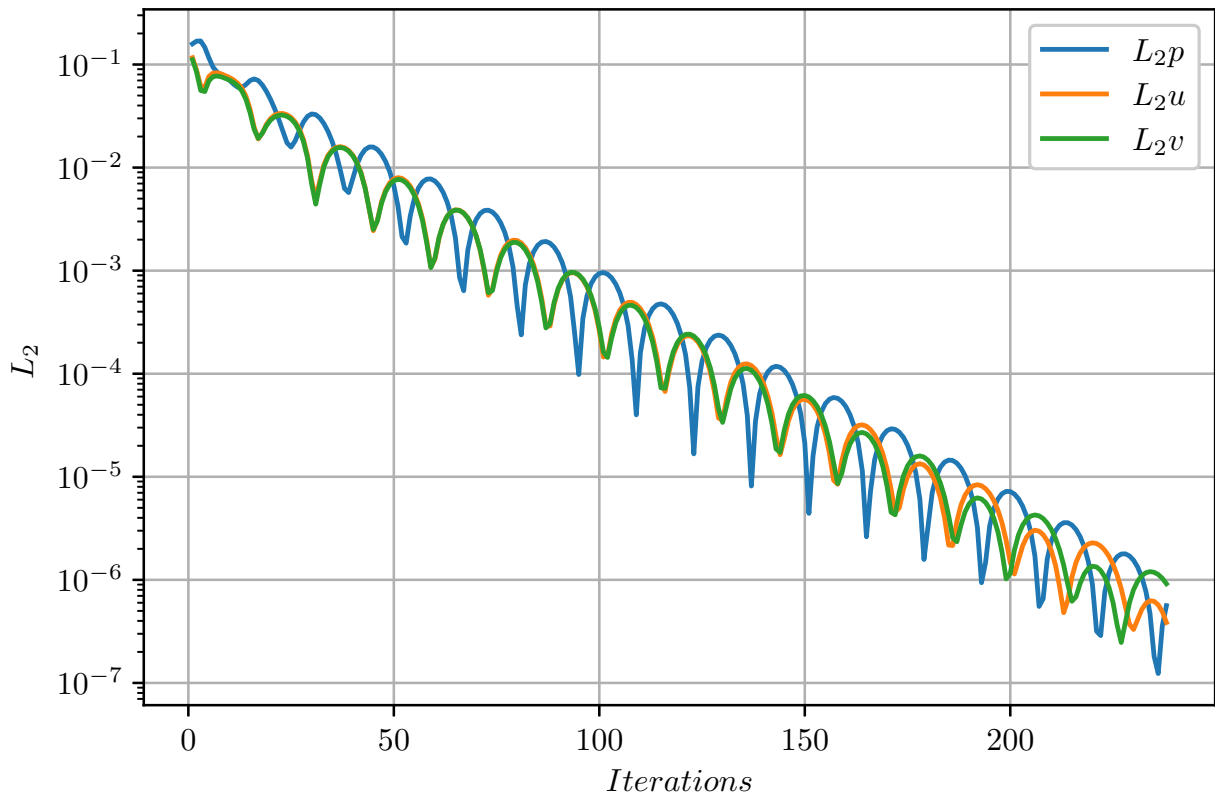


Figure 6: Convergence history for $U = 0$, $\Delta t = 0.05$, and 20×20 mesh Implicit method

For $\Delta t = 0.05$ the Explicit method was not stable, but it was stable for $\Delta t = 0.04$.

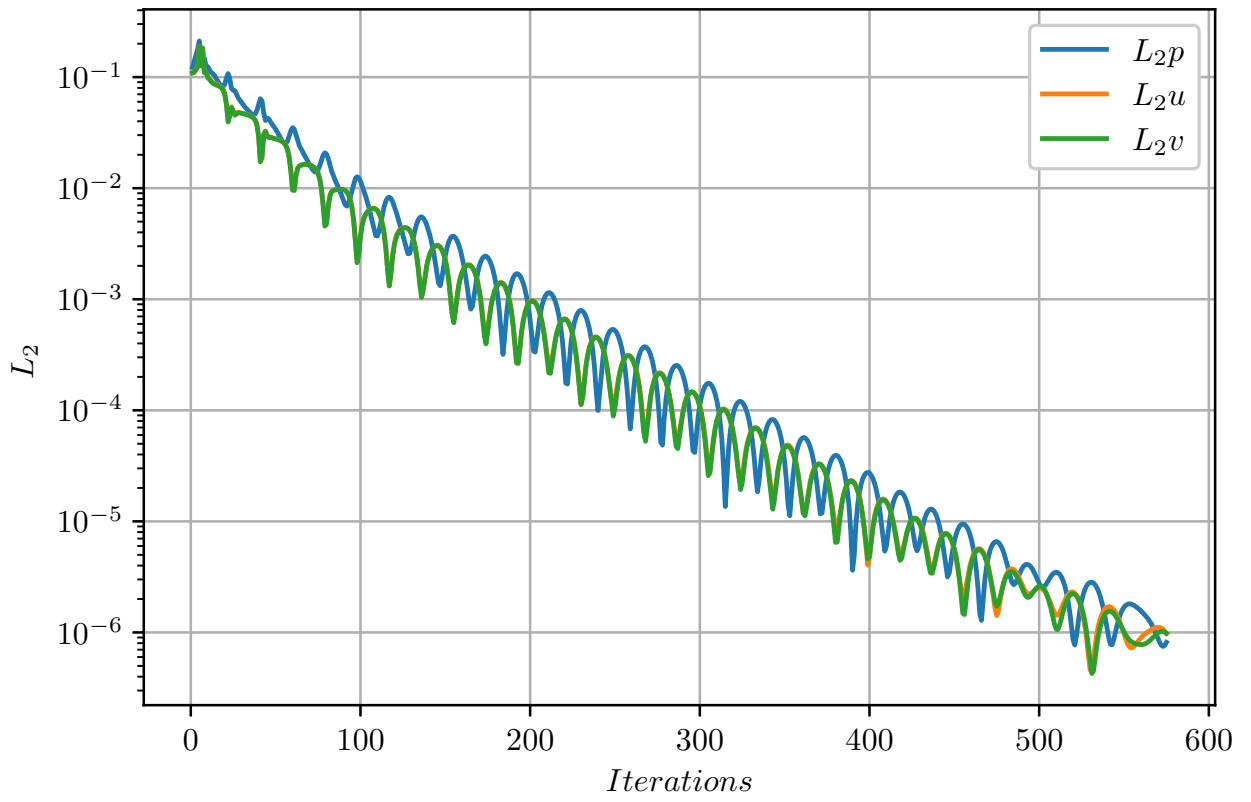


Figure 7: Convergence history for $U = 0$, $\Delta t = 0.04$, and 20×20 mesh Explicit method

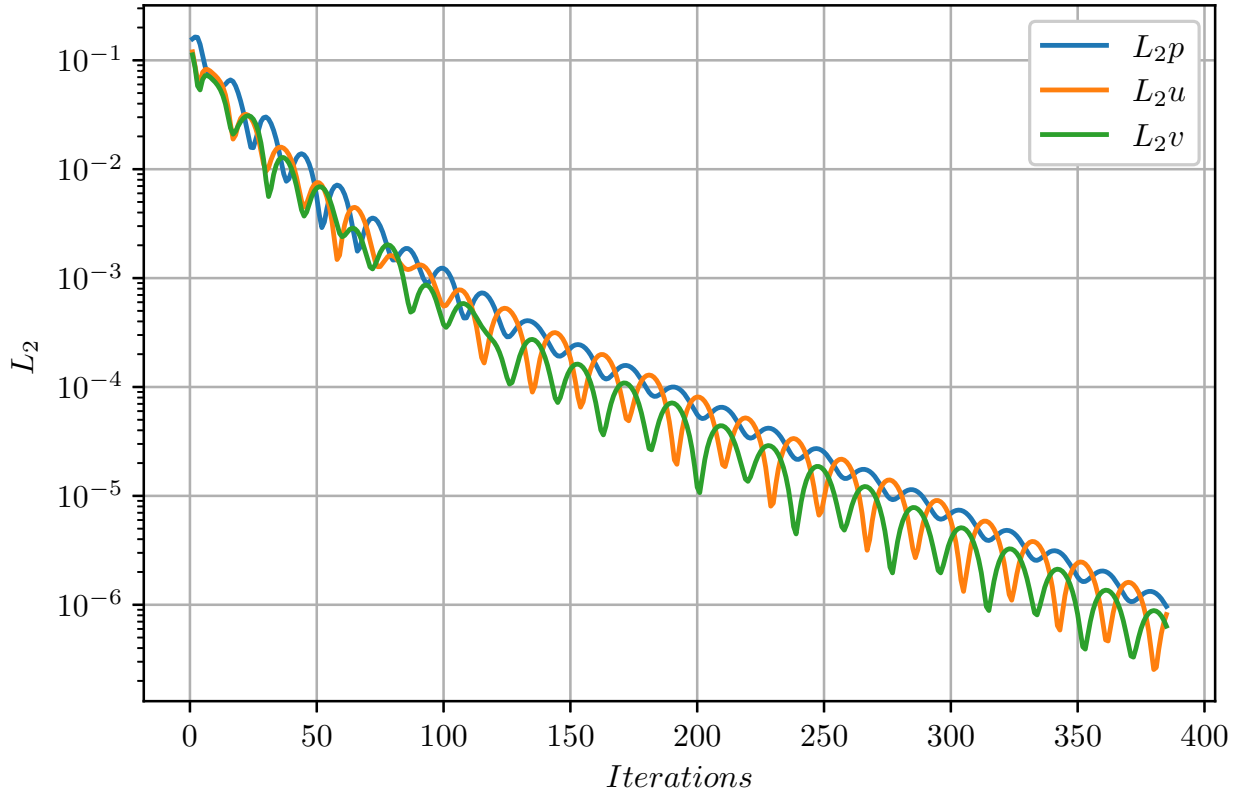


Figure 8: Convergence history for $U = 0$, $\Delta t = 0.04$, and 20×20 mesh Implicit method

As we see in Fig.6 Implicit method with $\Delta t = 0.05$, converges with smaller number of iterations. For comparison of Explicit and Implicit methods we had to choose smaller time steps (i.e., smaller Δt), since Explicit method is not convergent for $\Delta t = 0.05$. For $\Delta t = 0.04$ the Implicit method Fig.8 is converged with smaller number of iterations than Explicit method Fig.7.

8.1.1 Choice of β

As we said β in Eq.(14) scales the effect of Pseudo Compressibility term, in this section we examine the best β to be selected:

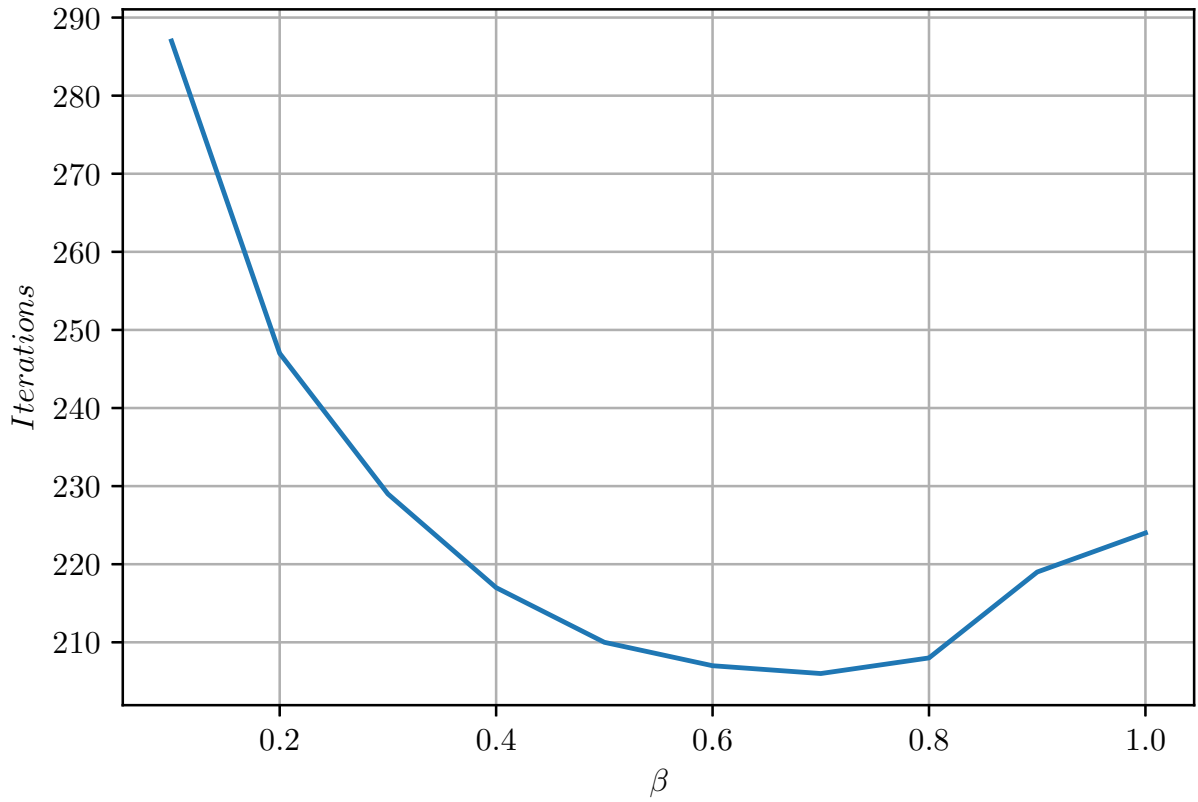


Figure 9: β vs number of iterations for 10×10 mesh and $U = 0$.

As we see in Fig.9, $\beta \approx 0.7$ is the best, but choose of β between 0.4 to 1.0 is still reasonable.

8.2 Basic Solution

8.2.1 Solution for $U = 1$

In this section we solve the Cavity Flow for $U = 1$ as it was described in Sec.1.2.1.2 for a 20×20 mesh, $Re = 100$, $\beta = 1$, $\Delta t = 0.05$, and $\Delta t = 0.01$.

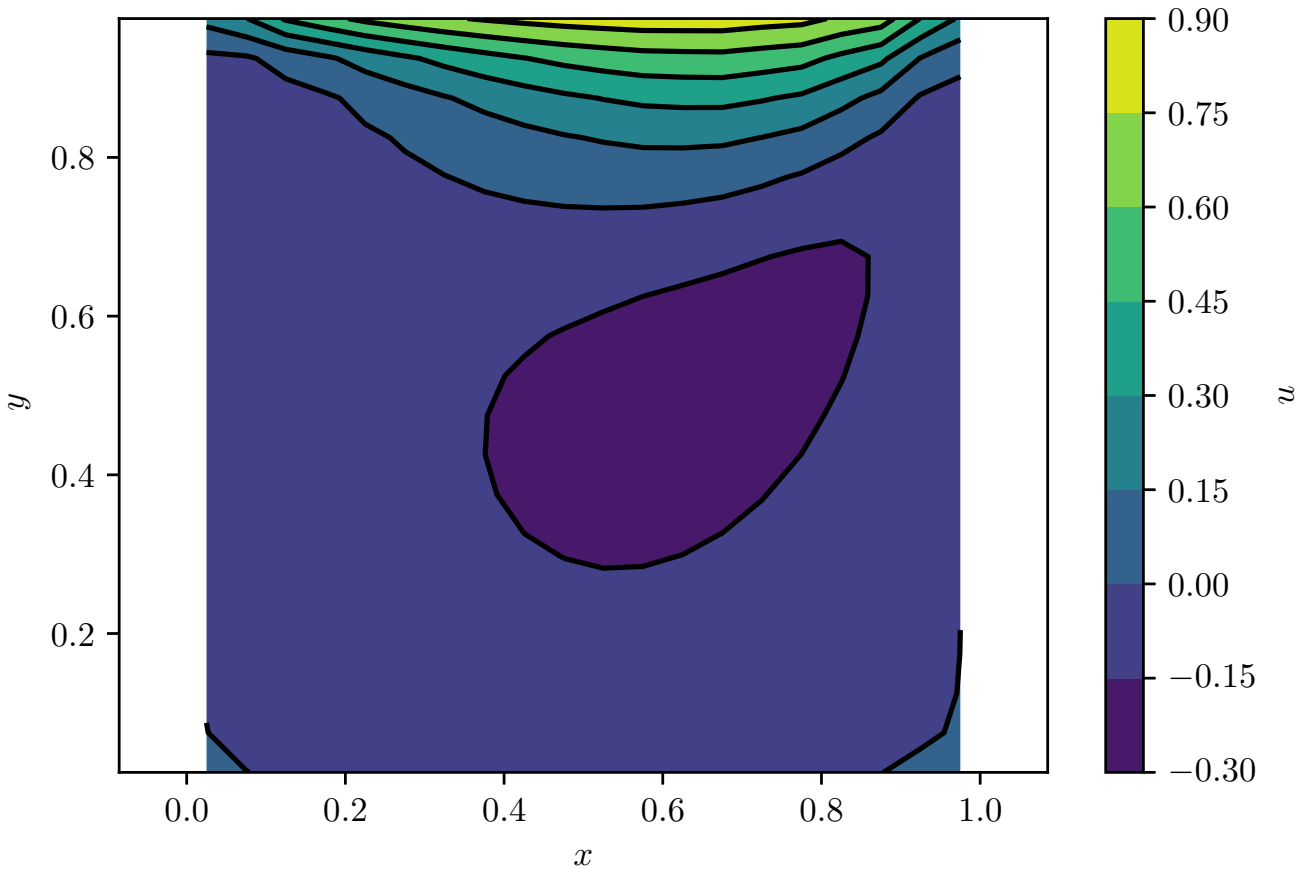


Figure 10: x -Velocity for $U = 1$, $\Delta t = 0.05$, and 20×20 mesh

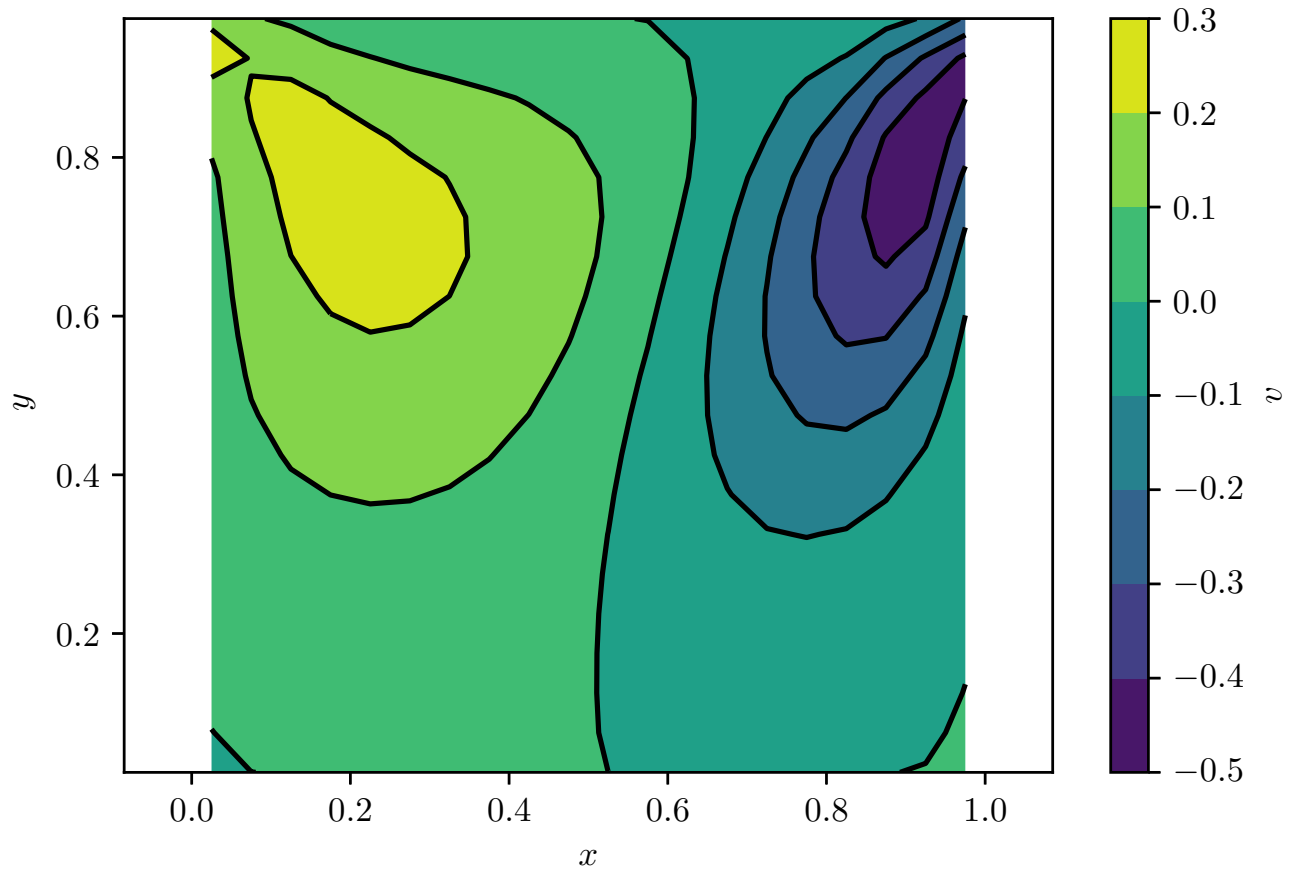


Figure 11: y -Velocity for $U = 1$, $\Delta t = 0.05$, and 20×20 mesh

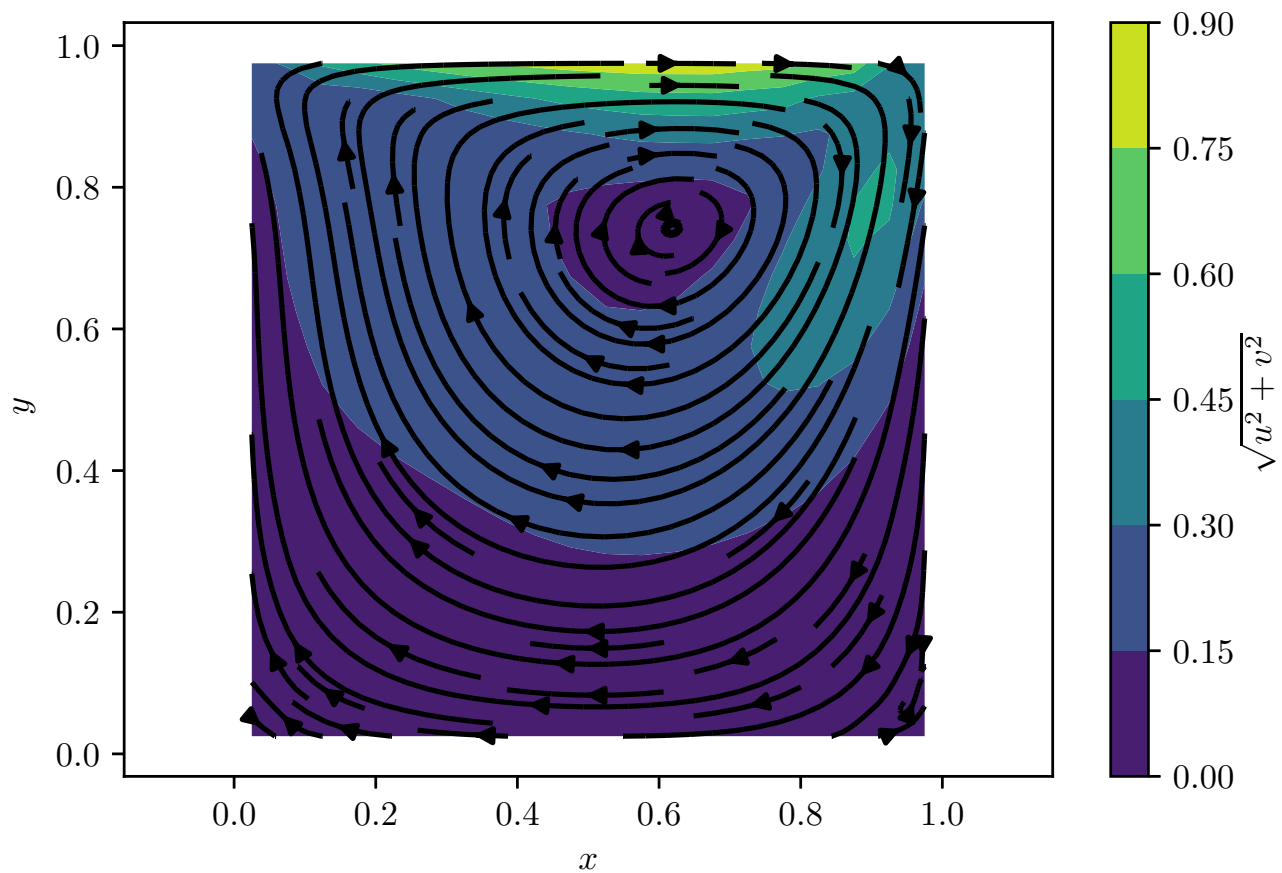


Figure 12: Absolute Velocity for $U = 1$, $\Delta t = 0.05$, and 20×20 mesh

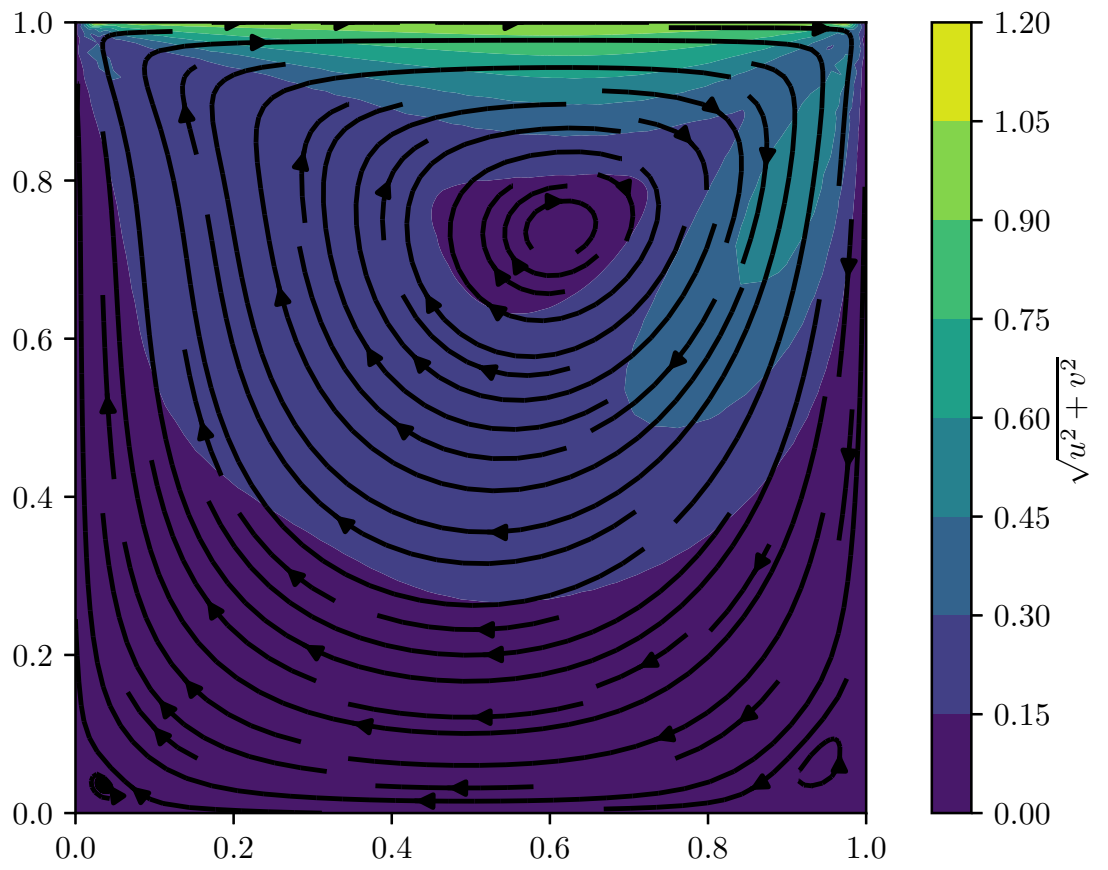


Figure 13: Streamlines of the cavity flow

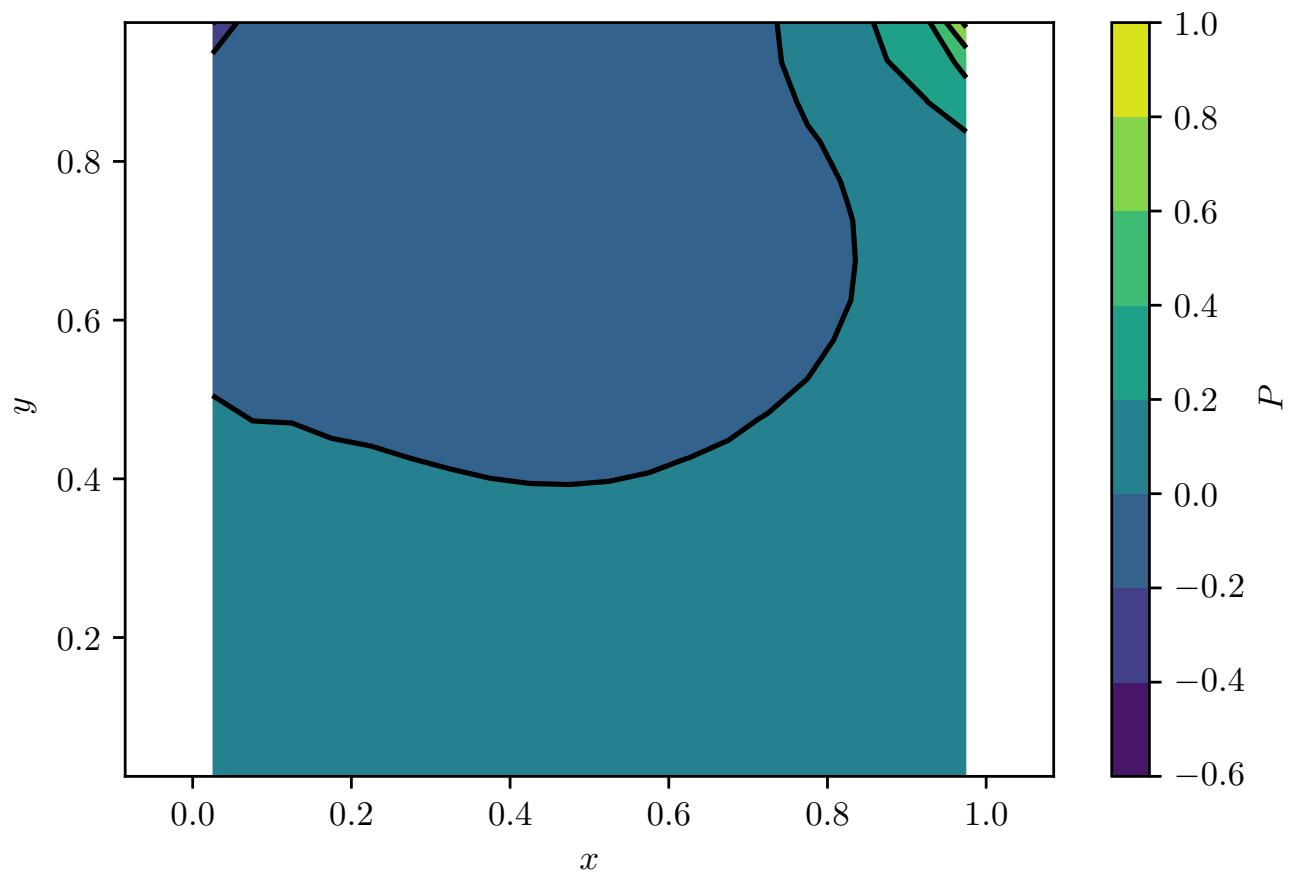


Figure 14: Pressure for $U = 1$, $\Delta t = 0.05$, and 20×20 mesh

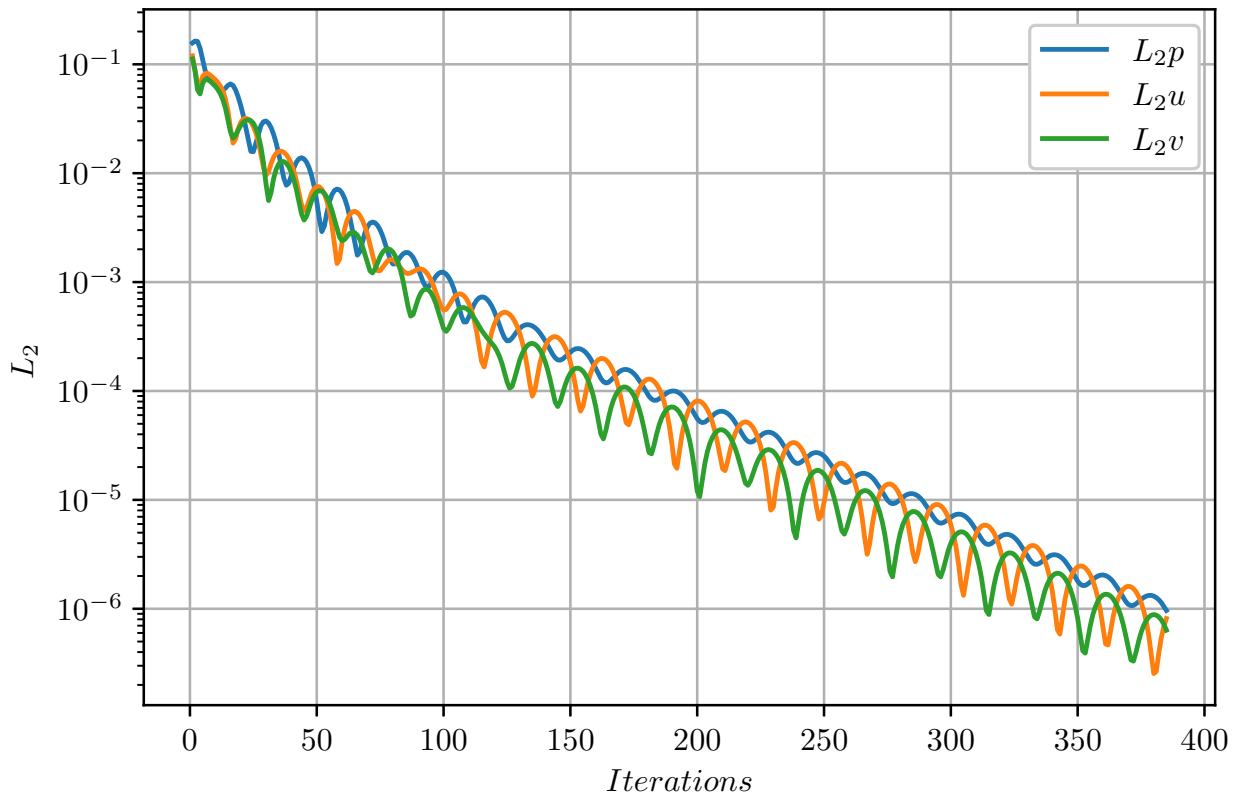


Figure 15: Convergence history for $U = 1$, $\Delta t = 0.05$, and 20×20 mesh Implicit method

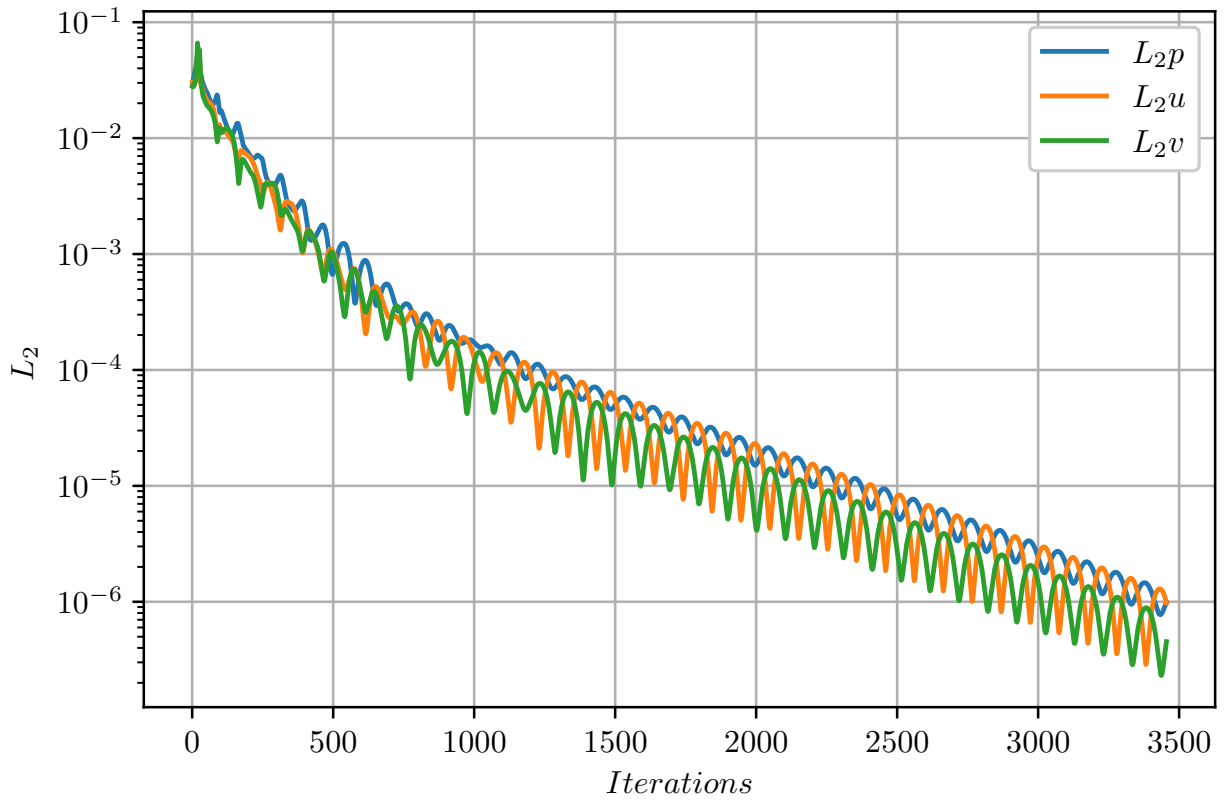


Figure 16: Convergence history for $U = 1$, $\Delta t = 0.01$, and 20×20 mesh Explicit method

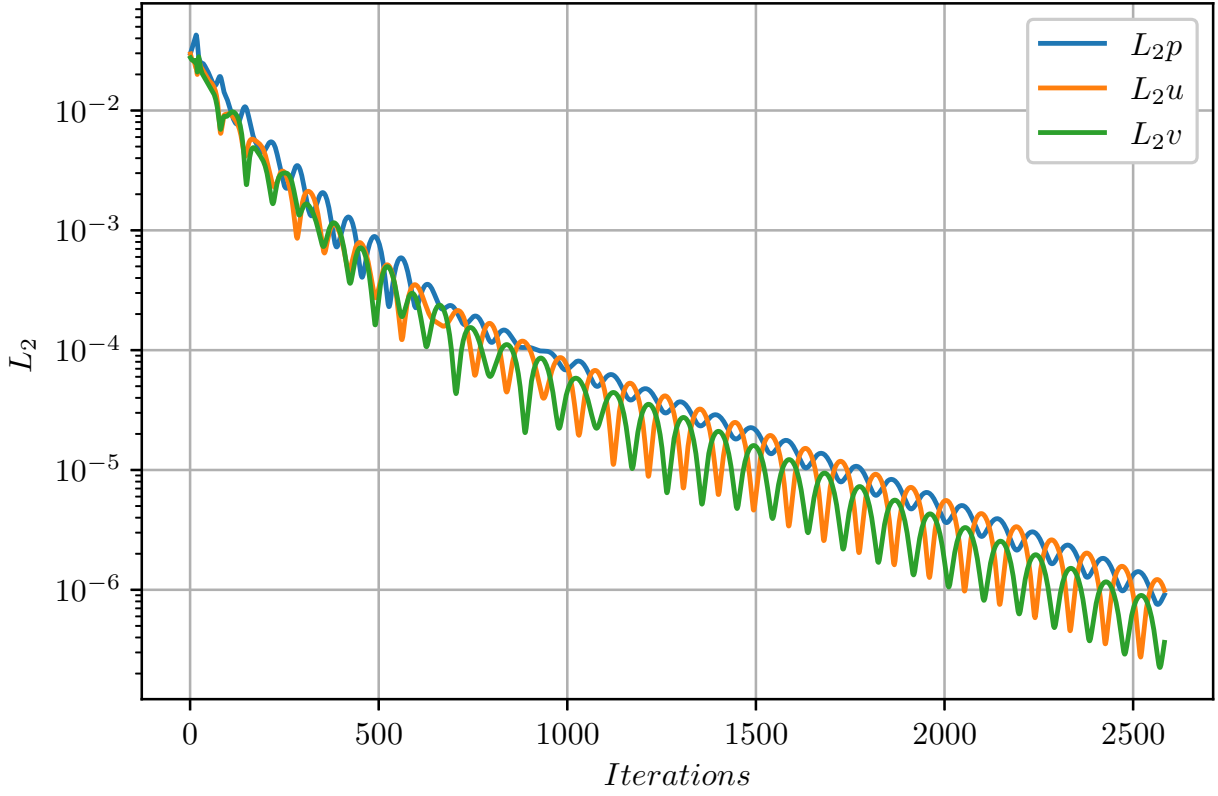


Figure 17: Convergence history for $U = 1$, $\Delta t = 0.01$, and 20×20 mesh Implicit method

It is clear that time step has a determinant effect on the number of iterations for convergence, and again from comparison of Fig.16 and Fig.17, Implicit method is faster than Explicit.

8.2.2 Sanity Check: Symmetry

In this section we have solved the problem for $U = -1$ as it was described in Sec.1.2.1.3. we calculate $u|_{U=1} + u|_{U=-1}$ and we expect it to be approximately zero everywhere.

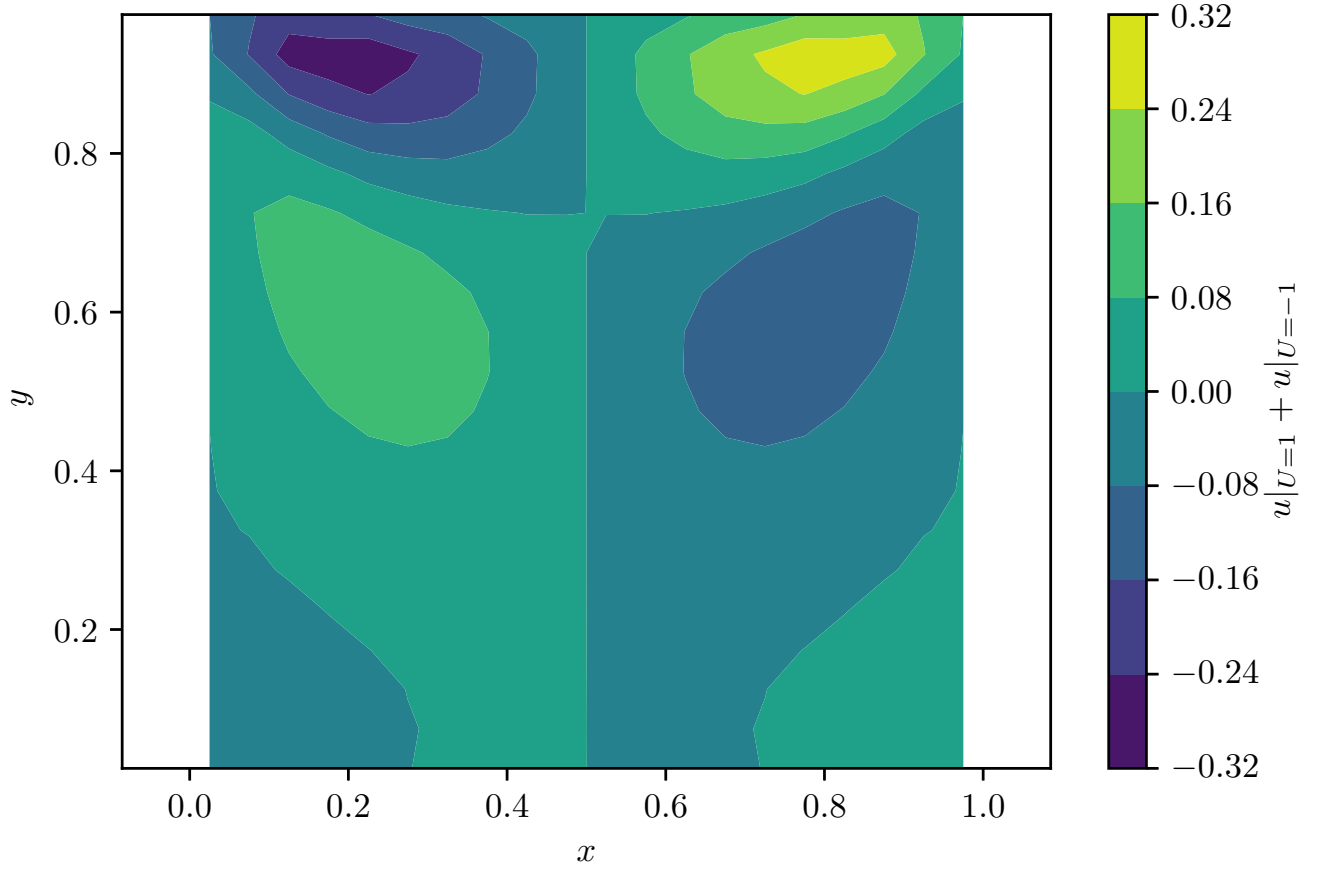


Figure 18: $u|_{U=1} + u|_{U=-1}$ for $Re = 100$, $\Delta t = 0.05$, and 20×20

As we expected in the Fig. 18 the x -velocity is approximately zero everywhere.

8.2.3 Grid Convergence

In this section we solved the Cavity Flow for $U = 1$, $Re = 100$, $\Delta t = 0.05$ as it was described in Sec. 1.2.1.2, for different mesh sizes and plotted the x -velocity on the symmetry line (i.e., at $x = 0.5$) and checked the grid convergence:

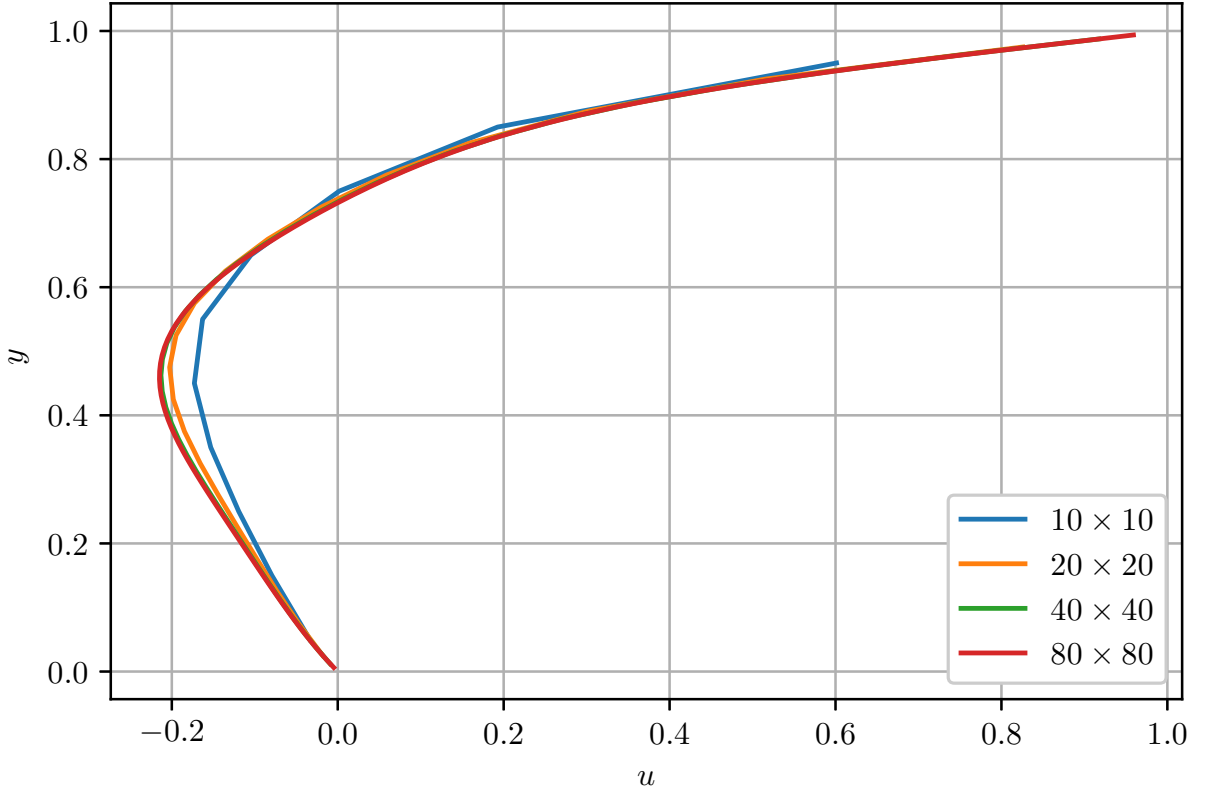


Figure 19: u at the symmetry line or $x = 0.5$ for $Re = 100$, $\Delta t = 0.05$, and different mesh sizes

As we see in Fig. 19, 20×20 mesh is converged enough for our examination, and for meshes smaller than 20×20 (40×40 and 80×80 in the Fig. 19) the curves collapsed to one curve.

8.3 Exploratory Case for Flow in a Box: Effect of Increasing h

As the height h of the box increases, the single vortex eventually becomes unstable, and a second vortex forms below it (and eventually a third, and so on). The exploratory part of this problem will focus on this formation of additional vortices with increasing h .

As it was described in Sec. 1.2.1.3 for $U = 1$, $w = 1$, $h = 3$, $Re = 100$, and $\Delta t = 0.05$, we have solved the Cavity Flow:

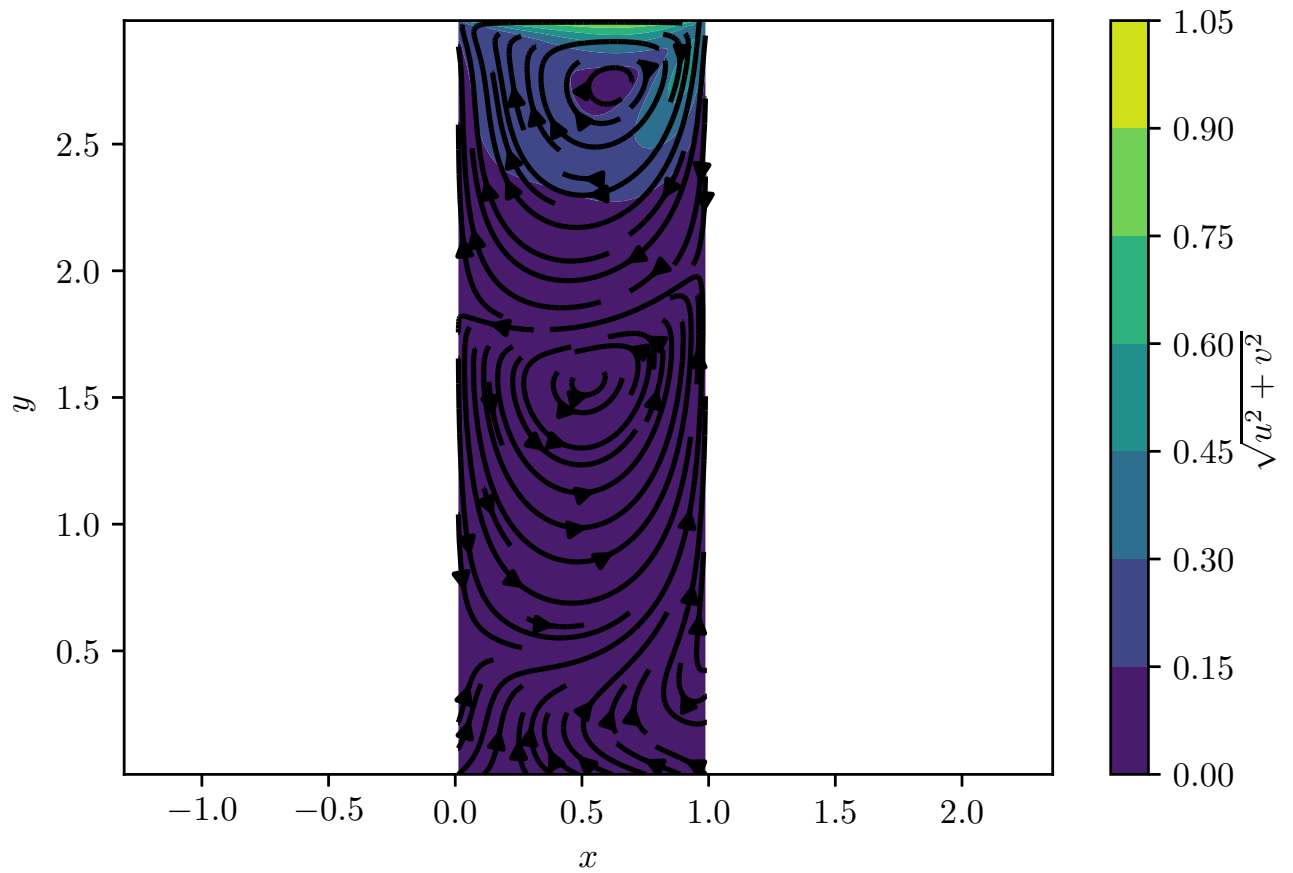


Figure 20: Vortices for increased height of the box

As we see in Fig.20 a second vortex is formed below the main vortex. If we increase the height of the box to 4 we will see a third vortex too:

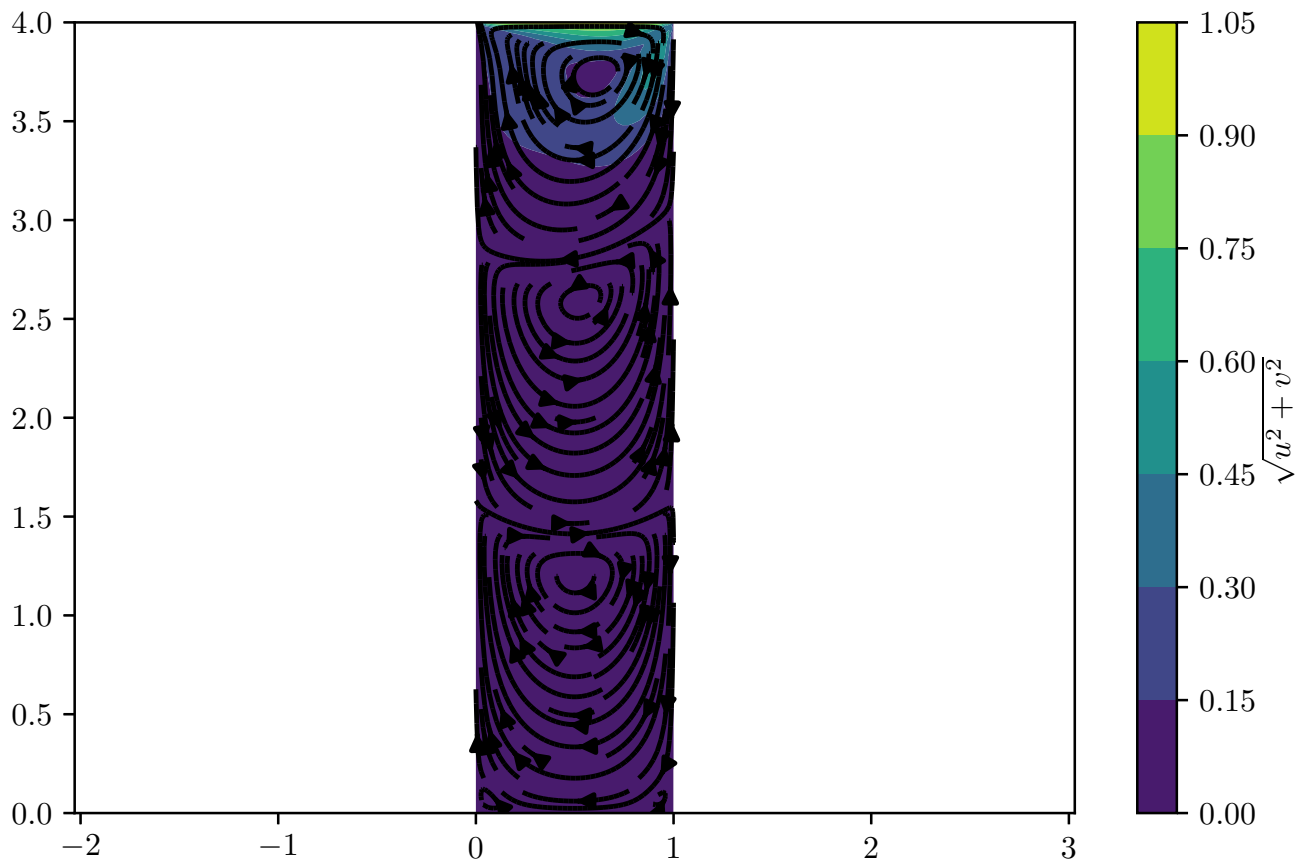


Figure 21: Emergence of third vortex in cavity flow

For the grid convergence we have solve the problem for 3 mesh sizes and plotted the x -velocity on the symmetry line:

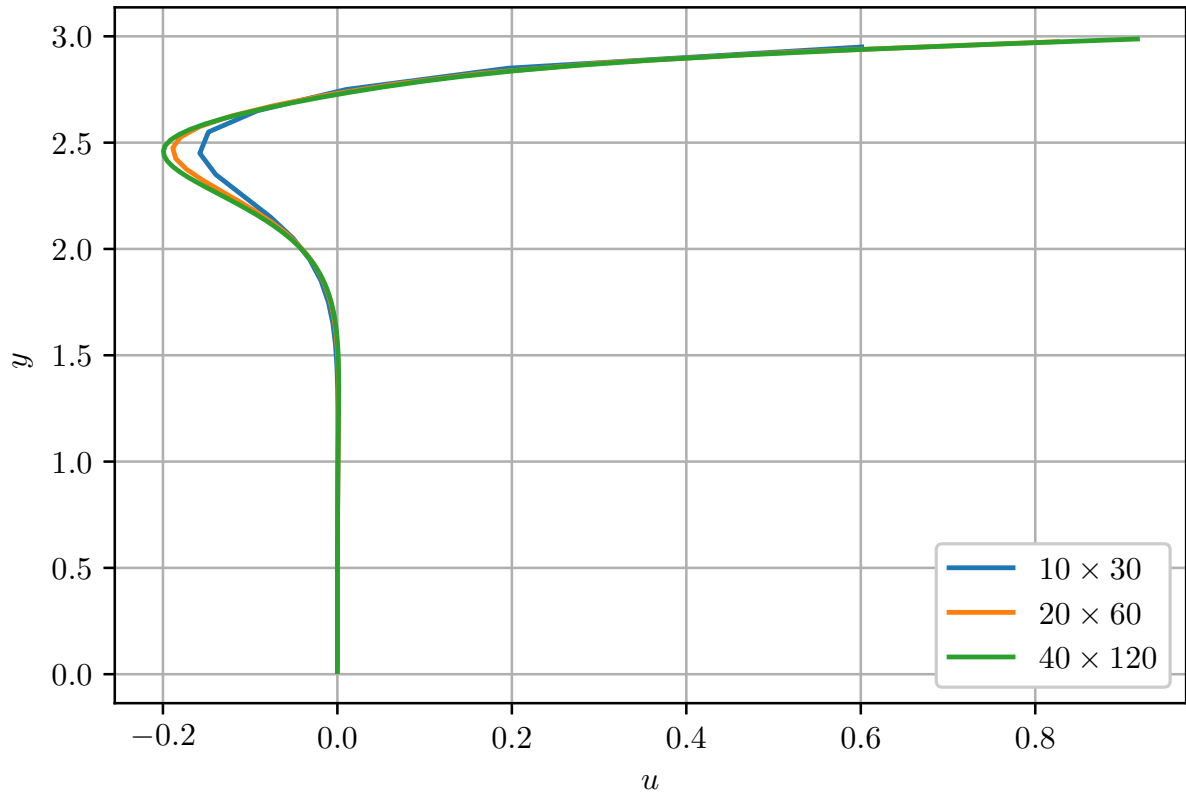


Figure 22: x -Velocity on the symmetry line ($x = 0.5$)

As we see in Fig. 22, 20×60 mesh is converged enough, we could not make the mesh size smaller than this because of the long time it takes for *python* to solve the problem.

8.4 Largest Stable Time Step for Explicit RK-4 Time Scheme

In the previous sections we compared Implicit and Explicit time schemes in this section we found the largest stable time step for RK-4 time scheme by using trial and error method.

Mesh Size	Δt_{max}
10×10	0.1
20×20	0.04
40×40	0.01
80×80	0.004
160×160	0.001

Table 6: Largest stable time step for RK-4 time scheme, $Re = 100$.

As we expected, in Table.6 the largest stable time step decreases as the mesh size increases.

9 Flow in a Duct with Inlet Velocity

In this case, we solve a flow inside a duct as it was described in Sec.1.2.2. The inlet velocity of $U = 1$ is set as the velocity inlet and the outlet pressure is set $p = 0$ as the gauge atmospheric pressure. The length and height of the duct are set to be 8 and 1 (everything is non-dimensional). The fixed pressure and fully developed condition are set as the outlet boundary conditions.

9.1 Solution of Duct Flow for a 20×10 and $Re = 50$

In this section we solved the problem for a 20×10 mesh, $Re = 50$, $\Delta t = 0.05$ and plotted the x -velocity at $x = 7$. We have calculated the x -velocity L_2 norm with respect to the exact solution.

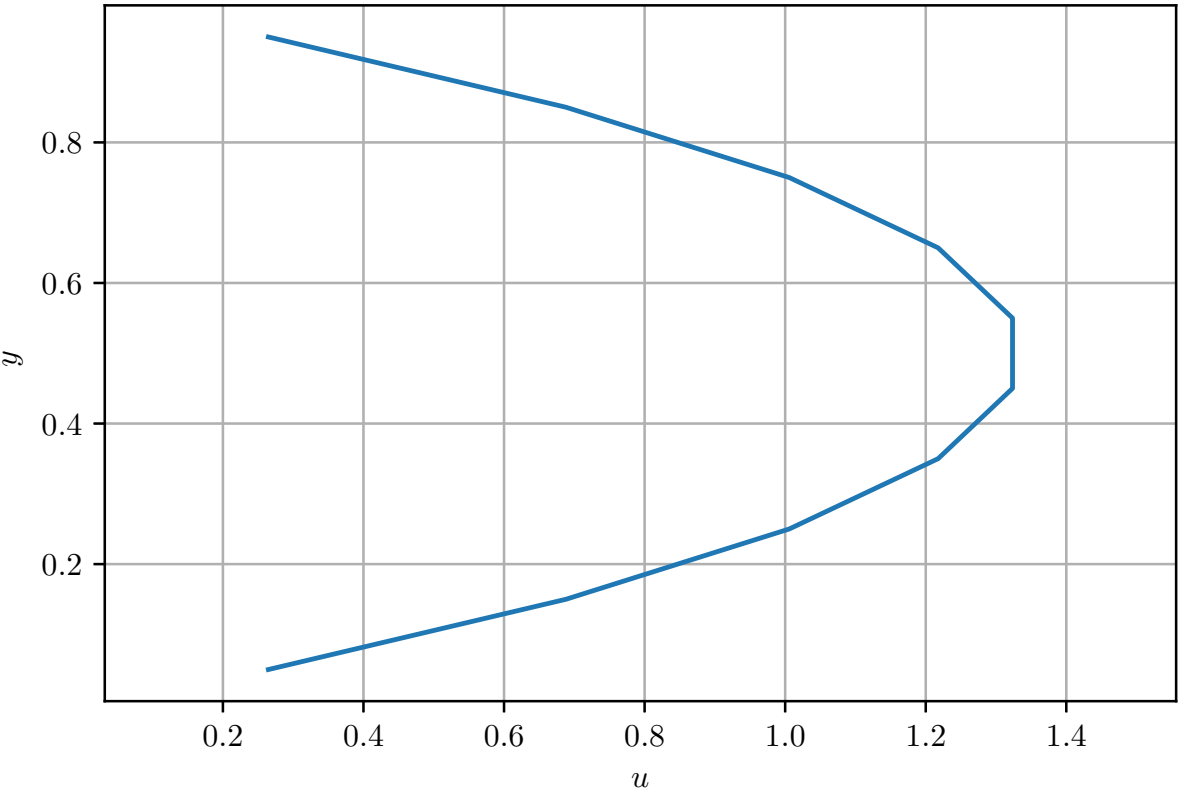


Figure 23: x -Velocity at $x = 7$

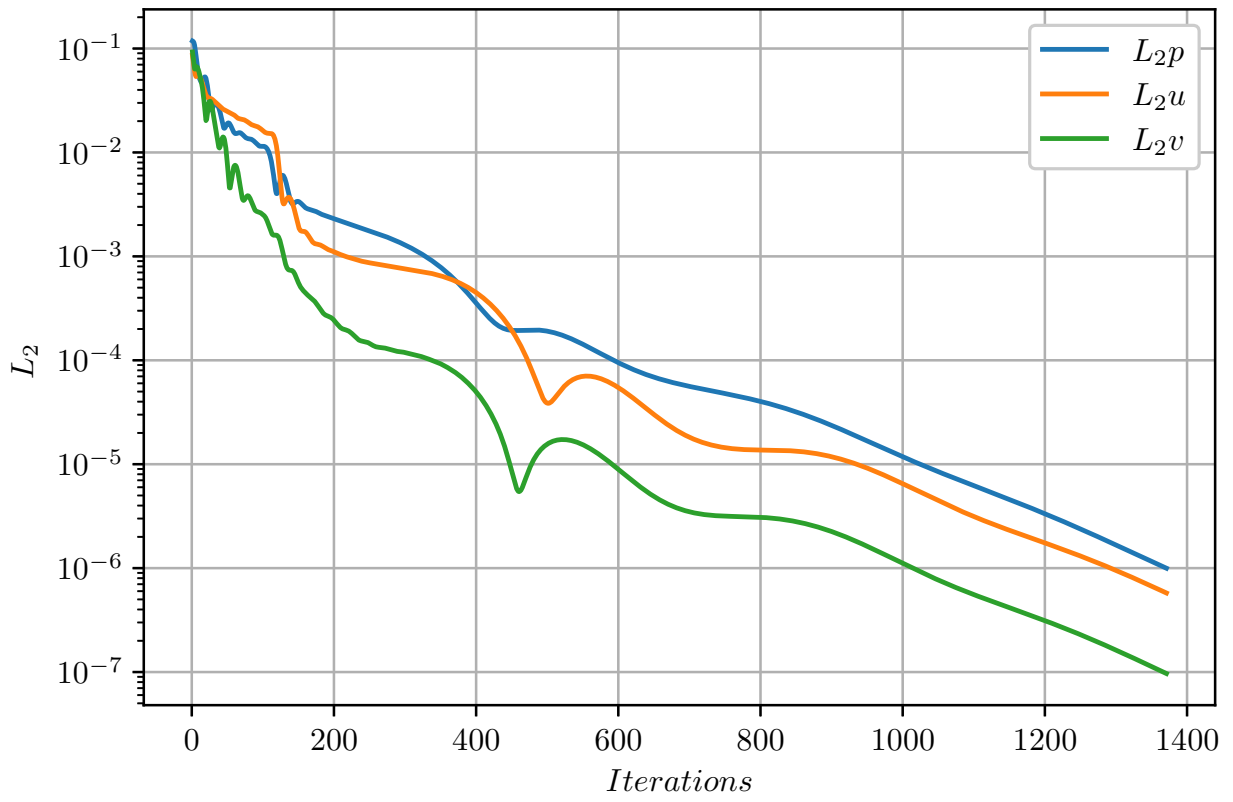


Figure 24: Convergence history Implicit time scheme

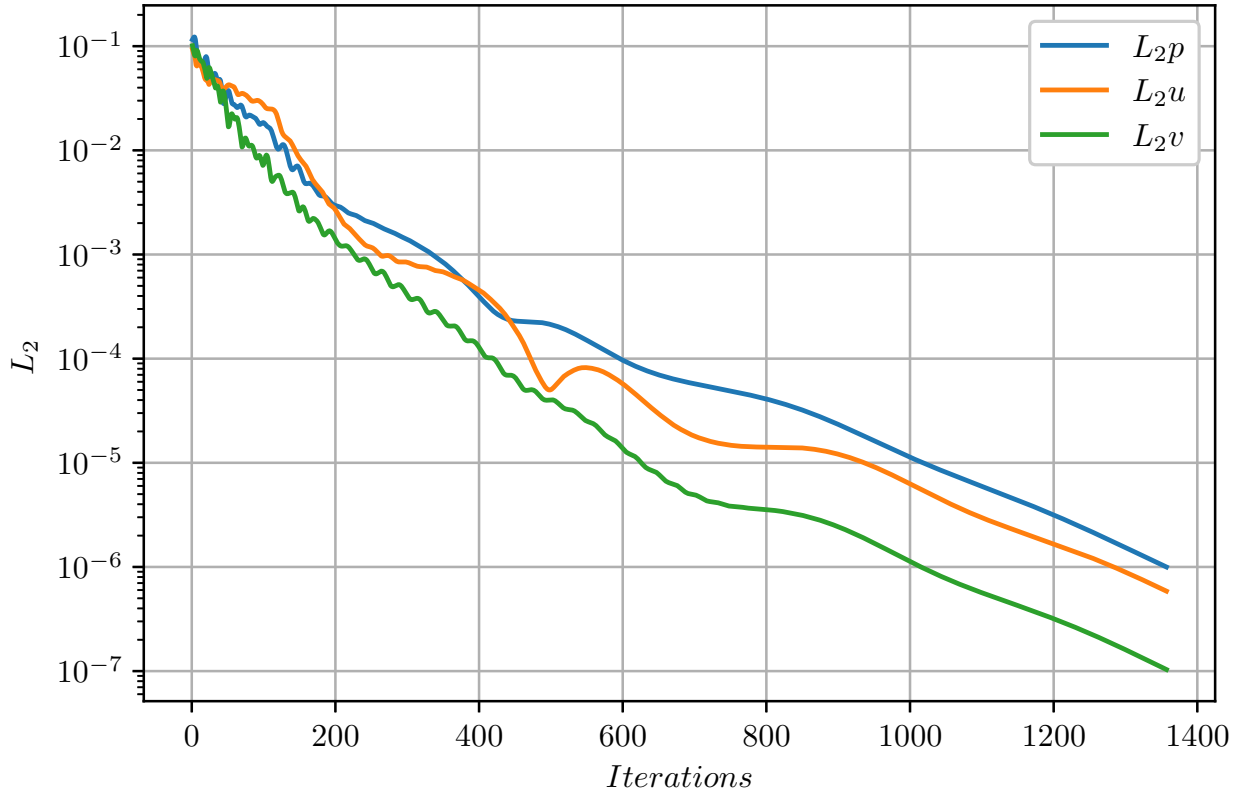


Figure 25: Convergence history Explicit time scheme

9.2 Grid Convergence and Explicit versus Implicit

In this section we repeated previous section for 40×20 and 80×40 mesh for the same Re number and compared x -velocity at $x = 7$ with fully developed non-dimensional Exact Solution as Eq.(66). Because of the long time it takes for python to compute the residual in each iteration and increasing number of iterations need for convergence we could not choose bigger mesh sizes than 80×40 .

$$u(x, y) = 6y(1 - y) \quad (66)$$

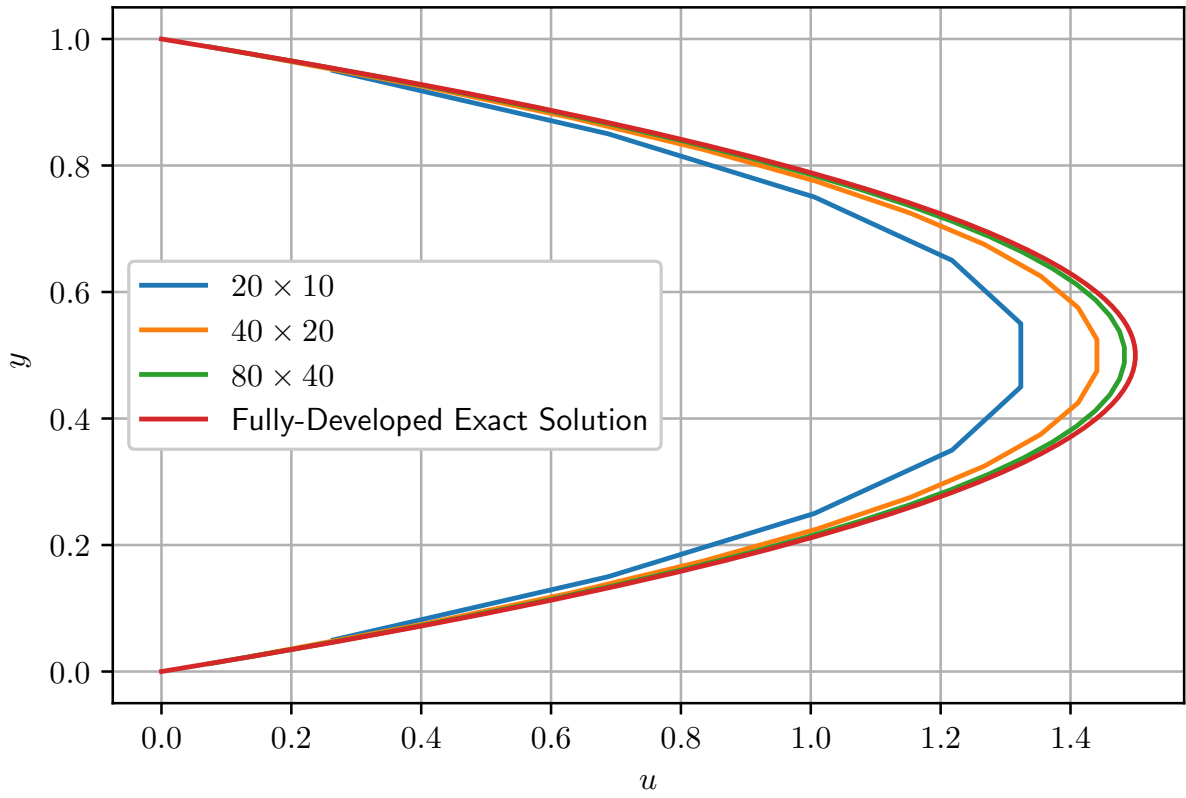


Figure 26: Velocity profiles at $x = 7$ for $Re = 50$

As we see in Fig.26 choice of smaller mesh length or bigger mesh size results in more accurate velocity profile. For mesh 80×40 the numerical solution converged to the Exact Solution satisfactorily. In the Fig.27 we can see the velocity field and streamlines in the duct flow:

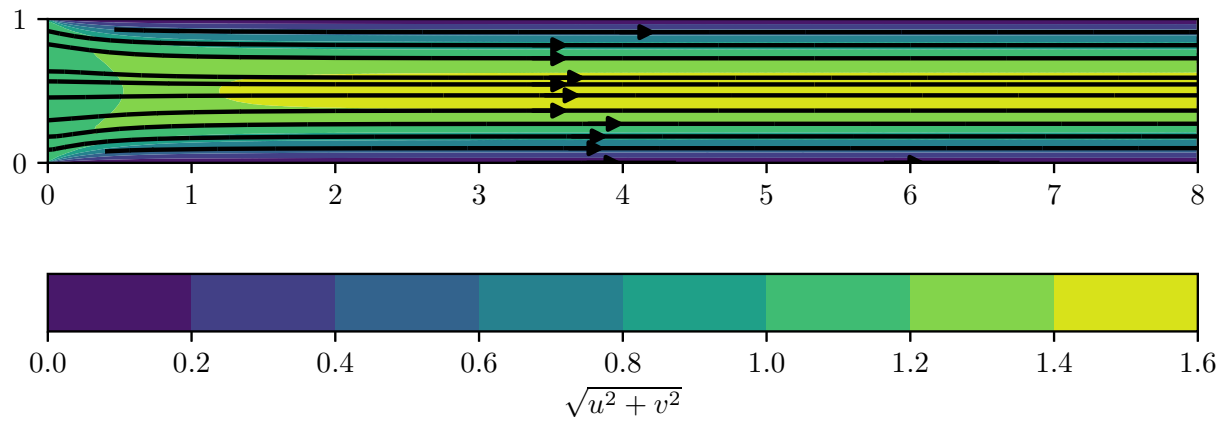


Figure 27: Velocity streamlines for duct flow

The choice of smaller mesh length results in smaller L_2u with respect to the exact solution Eq.(66), this fact is being seen in the Table.7.

Mesh Size	L_2u
20×10	0.008419922
40×20	0.004667914
80×40	0.001302647

Table 7: L_2 norms of x -velocity respect to the exact solution Eq.(66) at $x = 10$, $Re = 50$

In the following you can see the convergence history for each mesh size and time scheme:

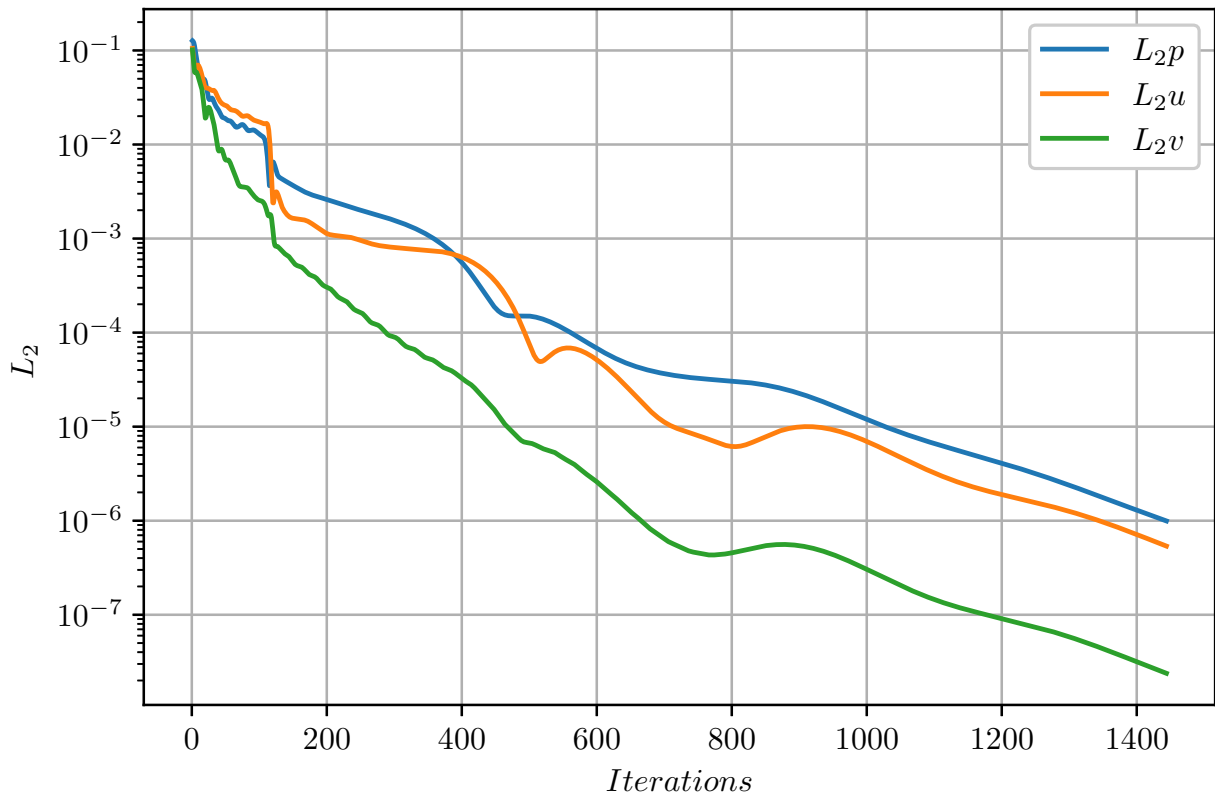


Figure 28: Convergence history Implicit time scheme for 20×10 mesh, $Re = 50$, $\Delta t = 0.05$

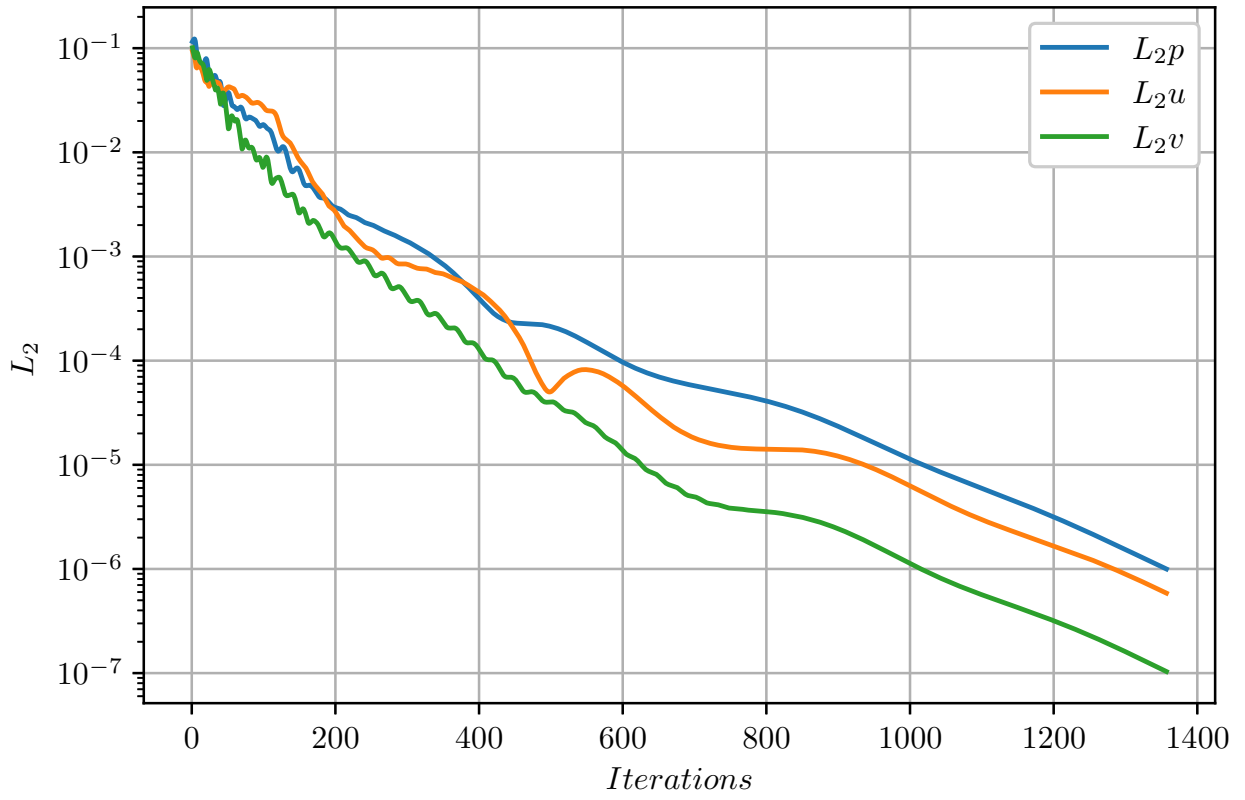


Figure 29: Convergence history Explicit time scheme for 20×10 mesh, $Re = 50$, $\Delta t = 0.05$

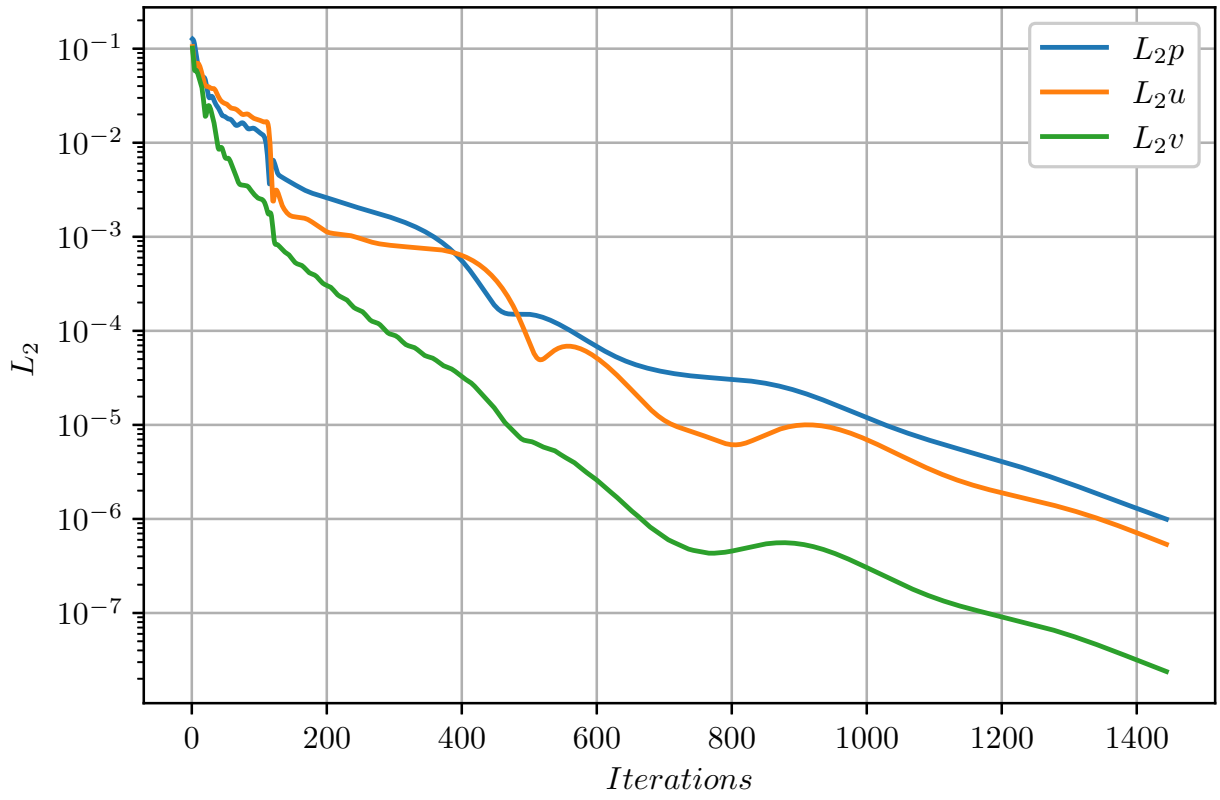


Figure 30: Convergence history Implicit time scheme for 40×20 mesh, $Re = 50$, $\Delta t = 0.05$

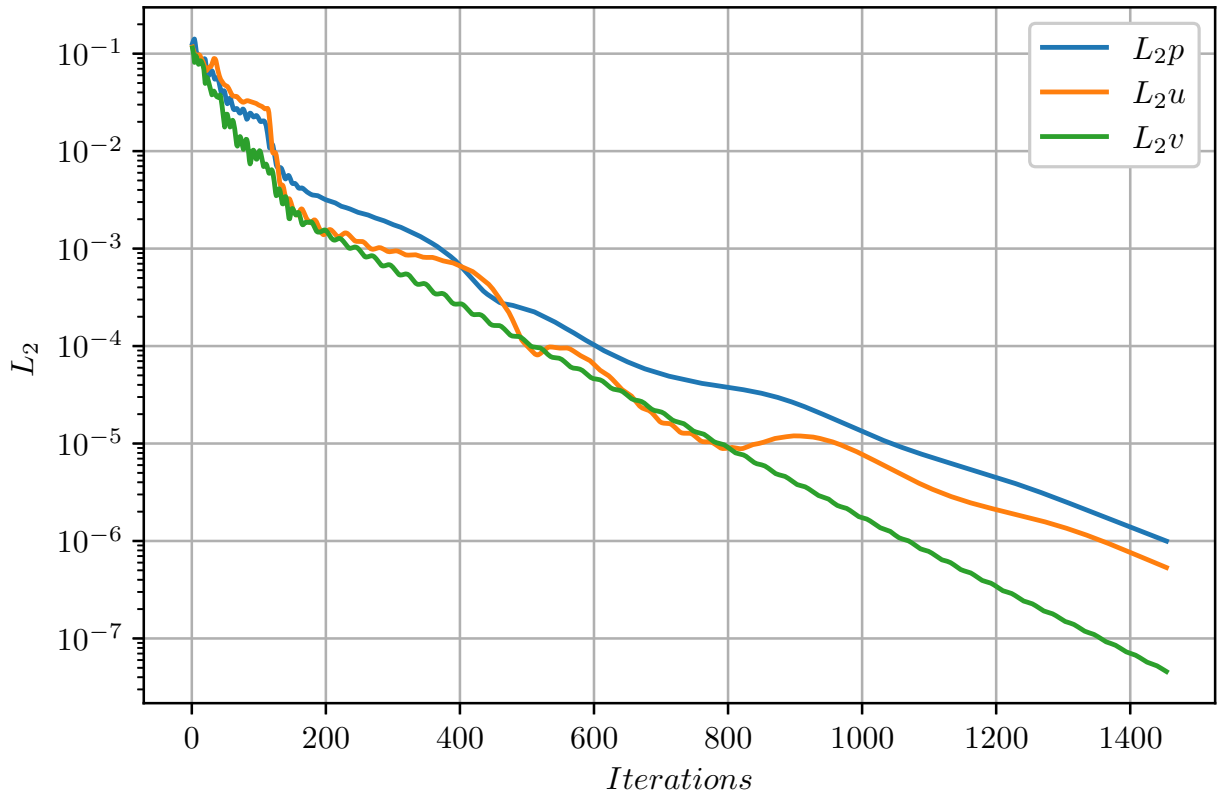


Figure 31: Convergence history Explicit time scheme for 40×20 mesh, $Re = 50$, $\Delta t = 0.05$

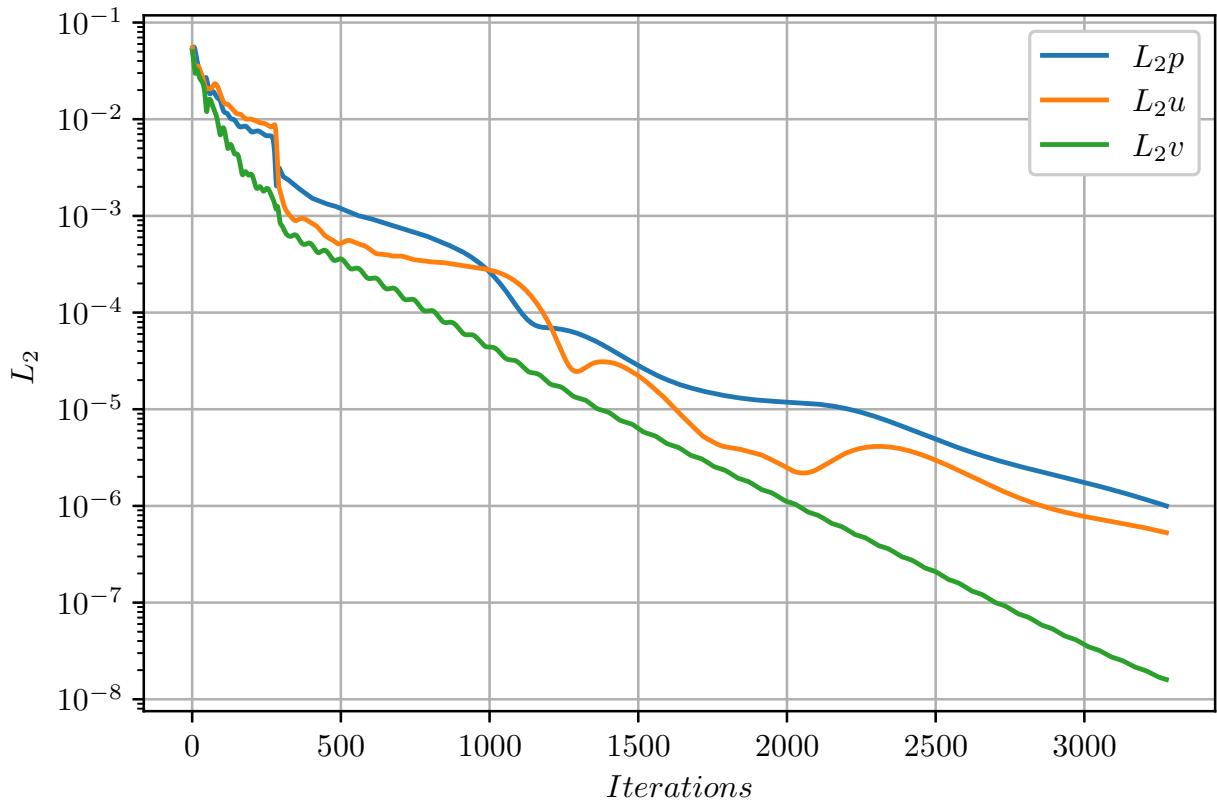


Figure 32: Convergence history Implicit time scheme for 80×40 mesh, $Re = 50$, $\Delta t = 0.02$

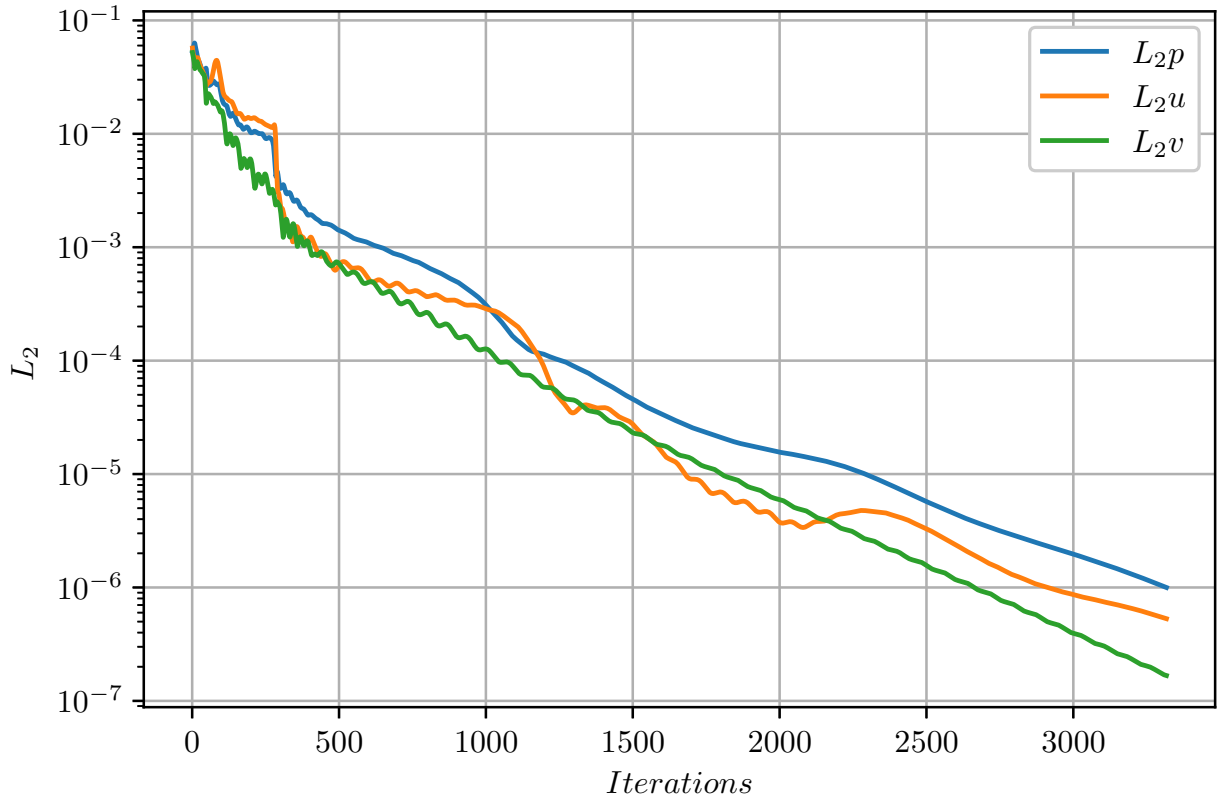


Figure 33: Convergence history Explicit time scheme for 80×40 mesh, $Re = 50$, $\Delta t = 0.02$

For CPU-Time comparison we have the following tables:

Mesh Size	Implicit CPU Time (s)	Explicit CPU Time (s)	Time Step
20×10	96.71875	47.828125	0.05
40×20	388.125	199.890625	0.05
80×40	3346.25	1768.78125	0.02

Table 8: Explicit versus Implicit CPU-Time comparison

This comparison in Table.8 have been done with time steps equal for both methods, but for Implicit method we do not have to choose small time steps as Table.8. We could select time steps as large as 0.1 for implicit time scheme as you see in Table.9:

Mesh Size	CPU Time (s)	Time Step
20×10	51.375	0.1
40×20	209.78125	0.1
80×40	828.140625	0.1

Table 9: Implicit time scheme with $\Delta t = 0.1$

10 Conclusion

In the present project we have solved incompressible Navier-Stokes equation using both Implicit and Explicit time schemes, the results showed higher speed of implicit method, additionally with implicit time scheme we can use larger time steps which can reduce convergence time significantly.